

Manuscript prepared for Clim. Past Discuss.
with version 2014/07/29 7.12 Copernicus papers of the \LaTeX class copernicus.cls.
Date: 2 July 2015

Scaling laws for perturbations in the ocean–atmosphere system following large CO₂ emissions

N. Towles, P. Olson, and A. Gnanadesikan

Department of Earth and Planetary Sciences, Johns Hopkins University, Baltimore, MD 21218, USA

Correspondence to: N. Towles (nathan.towles@gmail.com)

1 Response to Reviewer 1

1.1 Reviewer 1 Major Comment 1

The authors use the LOSCAR multi-box model of Zeebe as the generator of carbon cycle response, so the scaling relationships they seek are not data-based but rather meant to present a simplification of what is otherwise a fairly complex model meant to capture C cycle interactions on various timescales, but with a fairly simple representation itself.

I think the paper largely accomplishes its objectives. The authors explore in detail one particular scenario of emissions amount and duration, and conclude that the (apparently) expected relationship between rate (Emission/Duration) and perturbation (e.g., of atmospheric CO₂ partial pressure). I think here the authors should be more explicit about why this relationship should have the form they state (where the exponents of the scaling relationship add to zero). They might start with a simple ODE e.g., $dCO_2/dt = V - k CO_2^{(1/n)}$ and show that $n = \alpha + \beta$, etc.

1.1.1 Response

The *long-term* steady state balance of atmospheric CO₂ is assumed to be set by the balance of CO₂ rates of input via background volcanic processes and the rates of removal via weathering of silicates and subsequent burial of marine carbonate sediments - (As discussed pg 97 lines 17-23 of original manuscript). This steady state balance is thought to be achieved on timescales >100kyr. Given that our simulations were all for emission durations ≤100kyr and the variety of timescales involved in the interactions between the different carbon reservoirs, there is no a-priori assurance that a scaling law should exist at all, much less one that would take form of a power law. We adopted the particular power law form because it lends itself to a simple interpretation of the long-term assumption of rate dependence eg E/D or $\alpha + \beta = 0$. Our twin goals are to (1) find out if power law scalings exist for large transient perturbations, and if so, (2) quantify how they differ from steady-state predictions. We have modified the introduction to make these objectives clear.

The symmetric-triangular shape of the emission scenario was adopted to facilitate observation and interpretation of peak system responses. As opposed to using a heavy-sided emissions shape with constant emissions rate, the symmetric triangular forcing provides a scenario where the peak rate of input occurs coincident with the time when 1/2 the total magnitude of emissions, at 1/2 the total duration of the event. We have added a statement to this effect.

1.2 Reviewer 1 Major Comment 2

The paper would have more utility if the authors could then show how this simplification of LOSCAR helps in the interpretation of or prediction of system response to a real-world perturbation. I'm not sure what to do with the scaling relationship, especially since it is derived from a fairly simple box model rather than observation.

1.2.1 Response

The scaling laws are intended to (hopefully) be used as a way to quickly estimate what particular emission-duration combinations one would need to produce particular peak changes in different parts of the earth-system. These could then be used as a starting point for a more complex, targeted, modeling assessment. In the supplementary material of the revised manuscript see the additional comparisons of scaling predictions to a more detailed assessment of expected peak changes due to those by realistic fossil fuel emission scenarios. Using the simple scaling relationships, one could have estimated the peak perturbations to total atmospheric carbon to (in the worst case) within (17%) of the full model results.

In order to develop scaling laws based on observations, one would first need to have quantitative data on the total magnitude of emissions and their duration as well as observations of peak changes in system variables, all of this for a range of emission sizes. In the case of modern fossil fuel emissions, we have information on our emissions, however we are not yet in a position to predict what the actual peak system perturbations will be.

For the case of past changes, we have some constraints on what the peak perturbations to different system variables were, but we typically rely on models to infer the information on the total magnitude and precise duration of the emission events that caused said perturbations. In other words, the reason to develop and use model-based scaling laws is that the observational record lacks critical pieces of information. We hope that the revised introduction now makes this point.

1.3 Reviewer 1 Comment 3

I believe the authors have mischaracterized the Genie model and its application by Ridgwell, Kump and colleagues to events like the PETM. Genie has a fully interactive sediment component, similar to that in LOSCAR but calculated at each benthic grid cell. It should be listed with the Bergen model on line 10 of page 98 as an Earth system model that fully simulates the carbonate part of the global carbon cycle.

The comparison to Genie results is incorrect because it apparently presumes that Genie doesn't have an interactive sediment module that can dissolve if overlain by under-saturated waters (or even over saturated waters, because CO₂ can be produced by aerobic decomposition in the sediments during early diagenesis).

1.3.1 Response

The revised manuscript has been updated to address these particular concerns.

1.4 Reviewer 1 Comment 4

The scaling relationships developed for d13C are based on a constant biological pump and carbon burial and thus do not allow for changes in the organic C part of the C cycle. This seriously compromises the ability of the model and the scaling relationships derived from it for fully capturing carbon cycle response to perturbation.

1.4.1 Response

As discussed on pg 112-113 of the original manuscript we agree that there are certainly additional important biological feedbacks that require further in-depth considerations; however, these considerations are beyond the scope of this present study. Additionally, as noted on pg 112 In 15-25, a robust connection between changes in the biological pump and climate remains uncertain. However, we do agree that this means one cannot blindly apply the scalings developed from one epoch to the scalings across Earth history. We hope that the revised manuscript now makes this point.

1.5 Reviewer 1 Comment 5

The comparison to Cui et al. also is a bit of apples and oranges because they (Cui et al.) have found that the isotopic composition of the carbonates that are being dissolved, for example, impacts the isotopic response of the ocean to a particular emission rate and composition. Without better knowledge of how this works in both models, a comparison of the two is likely to be misleading and mis-interpreted.

1.5.1 Response

After further review we agree that this comparison may be potentially misleading and has thus been removed in the revised manuscript. The comparison of the aforementioned fossil fuel scenarios in the added supplementary material will instead serve as one example of the utility of the scaling laws when comparing with detailed modeling results.

1.6 Reviewer 1 Minor Comments

The authors should refer to "steady state" rather than "equilibrium" to avoid unnecessary confusion with true chemical equilibrium when referring to model states.

Line 19 on page 111 should read deep ocean pH DECREASES, right?

1.6.1 Response

- These corrections have been implemented in the revised manuscript.

2 Response to Reviewer 2

2.1 Reviewer 2 Major Comment 1

5 *I am confused about what seems to be the underlying precis or null hypothesis, of the*
paper - that of "simplified equilibrium considerations". Why, in a <100 kyr time-dependent
response, would anyone assume a behavior completely consistent with "the long-term
equilibrium between CO₂ input by volcanism and CO₂ removal by silicate weathering".
The clue here is that estimates for the time-constant of "the long-term equilibrium between
10 *CO₂ input by volcanism and CO₂ removal by silicate weathering" start at about 200 kyr,*
and some even longer than this (in LOSCAR, it is not complete even by 1 Myr). Why would
something occurring transiently on e.g. order 10 kyr conform to a the end result of a process
that requires the best part of 1 million years to complete? Hence I just completely don't get
this argument - it makes absolutely no sense but pervades the entire manuscript (starting
15 *with the Abstract text) and sets the agenda (i.e. null hypothesis). Maybe it just needs to be*
*explained *much* better, but more likely, I don't see such thinking as having a logical part*
to play in the paper. (The study and analysis is perfectly justifiable without what seems like
the creation of a false controversy.)

2.1.1 Response

20 As the referee correctly points out, given that our simulations were all for emission durations
 ≤ 100 kyr and in light of the variety of timescales involved in the interactions between
the different carbon reservoirs, it seems unlikely that equilibrium balances would apply to
transient emission events. Nevertheless, equilibrium assumptions have often been used to
interpret climate change signals, even in cases where the signal is clearly a transient. In

5 addition, the classical emission-weathering flux equilibrium is one of the very few balances that is simple enough and objective enough to offer quantitatively testable predictions. It is for these reasons we chose to include it as our straw man. That said, we take the referees' point that it was over-emphasized in our original submission. Accordingly, we have deleted its reference from the abstract and from most places in the text, but retaining it as part of the motivation discussion in the introduction.

2.2 Reviewer 2 Major Comment 2

10 *I appreciate the reasoning for adopting an abstracted and conceptual shape for the carbon emissions (one could chose a whole variety of alternative shapes such as pulses, but the primary findings of the study would likely be largely unchanged). What is missing however is a better connection to reality and essentially, a test of the predictions of the authors' "empirical" (in the sense that the model is based on a fit, but not on experimental or observational data) model for global environmental change in response to carbon emissions. What I am thinking of specifically, and strongly feel that is needed, is a test of the*
15 *empirical description against an anthropogenic fossil fuel emissions scenario, or scenarios (run using LOSCAR and potentially also contrasted to other model projections). I'll leave it up to the authors quite what emissions scenario to take. Obviously, emissions should follow historical reconstructions up until 2010 or 2014 or thereabouts. For terminating the emissions scenario, commonly people create a linear decline with the rate of decline chosen*
20 *to create a specific total of emissions (e.g. 3000 PgC). One could also apply a logistic curve to represent historical and future emissions (e.g. see Caldeira and Wickett [2005]). I expect (hope for!) a relatively good correspondence between the authors' empirical predictions and the explicitly run scenarios given that typical fossil fuel CO₂ emission scenarios have a shape not entirely unlike the authors' assumed form (Figure 1a).*

25 *However, other emissions scenarios and particularly geological carbon release episodes might not be as easily representable in a simple symmetrical linear up/down form. Knowing then on what time-scale and for what environmental parameters, the empirical model deviates most from explicit projection, is important. The easiest scenario for the authors*

to pick in this context would be the PETM LOSCAR scenario of Zeebe et al. [2009] (Nature Geoscience). Comparison of empirical model with the actual results of a more complex shape of emissions will help outline a possible "worst case" scenario for the applicability of the authors analysis. Note the additional (but scientifically rather healthy) challenge posed by the change with time of assumed carbon sources and hence $\delta^{13}\text{C}$ values in Zeebe et al. [2009]. For both these tests of the empirical model, misfits (anomalies) for key environmental variables should be calculated and appropriate discussion added. One might attempt to place some sort of confidence limits (though they will not be formal, statistical, numbers) on the model.

2.2.1 Response

We hope that the supplementary material (now included with the revised manuscript) provides the appropriate comparisons with realistic fossil fuel emission scenarios as suggested above. Additionally, we hope that the inclusion of our scaling analysis for the paleo version of LOSCAR and the corresponding discussion regarding the differences between the two configurations will provide useful insight on how scalings may be applied across different geological time periods. As discussed in the revised manuscript, future studies are required to investigate these important questions further.

2.3 Reviewer 2 Major Comment 3

I have some doubts about much of the analytical analysis presented in the Discussion, which at the outset, states the key assumption: "This approximation is only valid when the aqueous CO_2 is small in comparison with the carbonate ion concentration, as it is in the modern ocean". Surely, the entire point of the overall study is assess the impacts of 'large' (first line of Introduction) and "up to 50,000 PgC" (Abstract) carbon emissions, where the assumption will be quickly invalidated. Secondly, a key focus of the paper is past events, when the ratio of $[\text{CO}_2]:[\text{CO}_2?]$ would almost certainly been much greater for much of the earlier Cenozoic and mid-late Mesozoic (both $p\text{CO}_2$ and $[\text{Ca}^{2+}]$ higher). I don't feel that

this analysis is essential to the paper, which could easily live without it, but if it is going to be done, it needs to be done properly. If the approximation turns out to be acceptable, then this needs to be demonstrated.

2.3.1 Response

- 5 In the revised manuscript (beginning on pg 15) we have rederived the equation without making the approximation at the outset. It turns out that the final answer, expressed in terms of the bicarbonate and carbonate ion concentrations, is identical.

2.4 Reviewer 2 Major Comment 4

- 10 *Lastly ... it needs to be clearer what the point of the paper is and, which might be the potential utility of the analytical expressions(?) I see this (provision of simple relationships to make forward projections of the maximum occurring global environmental change in response to massive carbon release, particularly in a paleo context) as a big plus of the paper.*

2.4.1 Response

- 15 We hope that the earlier discussion and the revisions/additions to the manuscript have clearly addressed these points.

2.5 Reviewer 2 Minor Comments

- 20 *page 96 / line 23 - Are 'super volcanoes' know sources of 'large' carbon emissions? (Maybe define or give some context to 'large', and appropriately reference throughout this sentence .)*

- Super volcanoes should not be considered large in the same sense as the other mentioned examples. This has been removed and proper context and references have

been added to the revised manuscript.

5 *page 97/98 - This is where the confusion is sown and a straw man created. I am not aware of long-term volcanic CO2 emissions/weathering equilibrium/balance assumptions, being applied to much shorter-scale transient situations.*

10 - We have carefully revised our wording of this. We did not mean to imply that this balance had been applied to shorter-scale transient situations. As mentioned above, our intent, was rather to question, if/how well this particular balance may be applied to these intermediate timescales (100 yrs - 100kyr).

15 *page 98/lines 5-17 - There are Earth system models of "intermediate complexity" too ... many if not most, include sediment interaction. You have sort of air-brushed out 10-15 years of modelling innovation at this point in the Introduction ;) However, you can still make the argument that for rapid assessment of events, particularly in order to explore a wide variety of emissions totals and time-scales, and potentially assess events analytically (using the equation), there is a need/role for simple (empirical) analysis.*

20 -It was not our intent to marginalize the importance of EMICs, but rather directly contrast the limitations of comprehensive models with simple models. We have more carefully explained our targeted message as it aligns with the final statement you made.

25 *page 100/lines 14-18 - Clarify whether modern or paleo configuration of LOSCAR. Regardless, in the Discussion, mention possible caveats to basing an empirical function on one particular configuration of climate and ocean circulation, whilst applying it to a different (configuration of climate and ocean circulation). (Unless you envisage having each set of equations being for a specific past time interval.)*

-This has been clarified to show that the study was using the modern configuration,

where applicable (considering that the paleo scaling have now been added). We also agree with your point about the possible caveats and have made revisions accordingly.

page 99 - I feel that the text of Section 2 would be better off as part of 'Methods'?

5 *page 100/lines 14-28+ ? There is some overlap with Section 2, and moreover, Section 2 would arguably make more sense in the context of having a summary description of LOSCAR precede it. (Hence I think merge the Sections.)*

10 -We agree with these suggestions and have reordered the text accordingly in the revised manuscript.

page 100-101 - An important caveat and need for extended Discussion, concerns the lack of explicit climate feedback in LOSCAR and what implications this might have for the subsequent analysis and empirical equation.

15 -We agree with this point and explicitly (pg 112 of original manuscript) alluded to these potentially important feedbacks that would warrant significant further analysis because the robust consideration these feedbacks is still uncertain.

20 *page 100-101 - In Methods, we are missing any description of the model spin-up used.*

- The model was in a known steady state (provided as the default modern configuration with LOSCAR). This can be seen in the results by looking at the 100yr run time prior to the onset of emissions.

25 *page 101/lines 15-18 -Perhaps clarify when the peak perturbation occurs relative to emissions peak and emissions end. (Given that you later vary the duration of emissions, it is not enough to know just when the emissions start.)*

- The chosen symmetric shape of our emissions scenarios means that the peak emissions always occurs at 1/2 the total duration. So knowing the total duration and when the peak perturbation occurs relative to emissions onset is all one needs.

5 *page 101/line 19 - Expand on what the "carbon tail phenomenon" is. "page 101/line 19-21 " I am pretty sure this is completely incorrect, but you do not describe exactly what in Archer et al. [2009] you are looking at. In general " given the short time-scale of the Archer et al. [2009] experiments (ca. 10 kyr) relative to silicate weathering (>100 kyr), the tail of the trajectories presented by Archer et al. [2009] will in general likely be dominated*
10 *by ocean-sediment interactions, and contrary to your statement about being "controlled primarily by silicate weathering fluxes".*

-Upon further review of our description we agree that our language could potentially be misunderstood regarding what we were referring to. We have updated our manuscript
15 to hopefully mitigate any unnecessary confusion about the connotations of the carbon tail.

page 102/line3 - You need to be much more careful with your wording here -total carbon, yes will be amplified, but not the effect on atmospheric pCO2 because of the linked increase in ocean ALK. (Buckets of potential for misreading of this and confusion.)
20 - The revised manuscript has been updated to to reflect this important clarification.

page 102/lines 14-15 - Define E(t).
- The revised manuscript has been updated to reflect this definition.

25 *page 102/line18 - I don't find Equation (4) as having any particularly useful meaning. Perhaps try expanding on its meaning and utility.*
page 103/lines 5-7 " Again, I am failing to appreciate what G'sys is telling me that I need to know.

- As briefly mentioned in pg102/ln19-21 (of the original manuscript) this tells the time dependent partitioning of carbon between the atmosphere and ocean reservoirs. To elaborate, after emissions onset a positive value <1 indicates that the atmosphere reservoir contains relatively more of the perturbation. The zero crossing indicates the time when the relative system response is equivalent in the atmosphere and ocean reservoirs. For negative values <-1 it means the system has amplified the perturbation and, if G_{atm} is always positive, all of the extra carbon in the system is located in the ocean reservoirs.

page 103 (and elsewhere) - When stating model years, think about whether these always need to be stated to the nearest single year, or an approximation would suffice.

- We have updated the manuscript to reflect approximations instead.

page 103/lines 8-15 - Would Ω not be more useful to show and discuss than TA as it has obvious and rather more direct paleo-environmental and ecological relevance? (Or show both.)

- We show TA because of its extensive use in the analysis contained in the Discussion section. The saturation state of course would be important if we were focusing on the characterization/interpretation of a response to a real-world event; however, the case study is there to give examples of the variety of LOSCAR outputs and an example of our interpretation of that information.

page 103/lines 17-20 - link to and reference the classic Zachos et al. Walvis Ridge / PETM paper. Also see Kump et al. [2009] (Ocean Acidification in Deep Time, Oceanography 22, 94-107).

- We have updated the manuscript to reflect the appropriate inclusion of the Zachos et al. reference.

page 103/line 25 - *Why not calculate a weighted mean? (There is no justification for taking an unweighed mean.)*

page 104/lines 20-21 ? *Please calculate weighted mean.*

- We have updated the manuscript to reflect the volume-weighted means where appropriate.

5

page 103/line 27 - *Typo (about the only one I spotted!) ? "temperatures" should not be plural.*

-This typo has been corrected.

10

page 104/line 26 - *These experiments did not seem to be explicitly detailed anywhere. Could we at least see time-series for emissions and one or two key environmental variables (e.g. pCO₂)?*

Table 1 - It would help to add columns detailing the values of D, E, R.

15

- The time-series in the case study results are for case 1 in the table. We do not feel that the addition of plots illustrating the higher 20000PgC case would aid in the overall interpretation of the results. However, the relevant E and D of each case was added to the table for clarification.

20

page 105-106 - *Hints of another straw man. Why would you expect the responses to be ?linear? and in ?proportion to E?? e.g. see Goodwin and Ridgwell [2010] (Ocean-atmosphere partitioning of anthropogenic carbon dioxide on multimillennial timescales, Global Biogeochem. Cycles 24).*

25

- The statement was not meant to indicate an expectation of linearity; however, it was meant to serve as a comparison of results to those that would be expected if the system produced linear results. We have rephrased this in the updated manuscript.

page 105/line 7 - No, because ALK (TA) also changes ...

-We believe that the reviewer means p. 106 here? We have largely moved this section to the introduction where we discuss what can be learned from equilibrium scaling laws in order to motivate exploring whether there are transient scaling laws.

5

page 107/lines 18-28 - make sure you fully explain why all of this might be of use/interest.

- We believe the above comments have addressed this, as well as , the updates in the revised manuscript.

10

page 111/line 19 - pH 'decreases' surely? Or technically: carbonate saturation decreases.

-This typo has been corrected.

Abstract

Scaling relationships are ~~derived for the~~ found for perturbations to atmosphere and ocean variables from large transient CO₂ emissions. Using the carbon cycle model LOSCAR (Zeebe et al., 2009; Zeebe, 2012b) we calculate perturbations to atmosphere temperature and total carbon, ocean temperature, total ocean carbon, pH, and alkalinity, marine sediment carbon, plus carbon-13 isotope anomalies in the ocean and atmosphere resulting from idealized CO₂ emission events. The peak perturbations in the atmosphere and ocean variables are then fit to power law functions of the form $\gamma D^\alpha E^\beta$, where D is the event duration, E is its total carbon emission, and γ is a coefficient. Good power law fits are obtained for most system variables for E up to 50 000 PgC and D up to 100 kyr. ~~However, these power laws deviate substantially from predictions based on simplified equilibrium considerations. For example, although~~ Although all of the peak perturbations increase with emission rate E/D , we find no evidence of emission rate-only scaling ~~$\alpha + \beta = 0$, a prediction of the long-term equilibrium between input by volcanism and removal by silicate weathering, $\alpha + \beta = 0$.~~ Instead, our scaling yields $\alpha + \beta \simeq 1$ for total ocean and atmosphere

25

carbon and $0 < \alpha + \beta < 1$ for most of the other system variables. ~~The deviations in these scaling laws from equilibrium predictions are mainly due to the multitude and diversity of time scales that govern the exchange of carbon between marine sediments, the ocean, and the atmosphere.~~

5 3 Introduction

The study of how the Earth system responds to large, transient carbon emissions is of particular importance for developing a better understanding of our past, present, and future climate. ~~Eruptions of super volcanoes,~~ Transient emissions related to extrusion of flood basalts ($10^2 - 10^4$ PgC (McKay et al., 2014)), dissociation of methane hydrates ($> 10^3$ PgC (Zachos et al., 2005; Zeebe et al., 2009)), and widespread anthropogenic burning of fossil fuels ($> 10^3$ PgC (Archer et al., 2009)) are a few examples ~~of these types of emissions.~~

What complicates our understanding of the response to these transient perturbations is the fact that there are many carbon reservoirs with a large range of intrinsic timescales associated with the different processes governing the Earth system. On timescales $< 10^3$ years, exchanges between the atmosphere, biosphere, soils and ocean occur. On time scales $10^3 - 10^5$ years, ocean carbonate-sediment interactions become significant (Archer et al., 2009). When dealing with timescales $> 10^5$ years it becomes necessary to consider effects of geologic processes such as silicate weathering, as these control how the system resets to an equilibrium a steady state balance. The complex interactions between so many system components over such a large range of timescales make it difficult to predict characterize how the Earth ~~responds~~ 's response to CO_2 perturbations of different magnitudes and durations has changed through deep time.

In general, the modeling of carbon perturbations is undertaken for two purposes. One is to predict future system changes that are expected to occur as a result of a particular emission history, such as the history of anthropogenic emissions in the industrial age. The other purpose is to infer the sizes and durations of carbon perturbations in the past, by

comparing model results with various recorders of environmental change. According to an often-used model based on simplified considerations of atmospheric equilibrium,

Scaling laws represent a powerful synthesis of important dynamics in many systems, illustrating in particular how different combinations of parameters may yield the same result, and highlighting particular parameters to which the solution is sensitive. In the model which we use here the *long-term* steady state balance of atmospheric CO₂ is assumed to be set by the long-term abundance of balance of CO₂ in the Earth system is determined by a balance between the injection of carbon into the atmosphere in the forms of volcanic and metamorphic emissions and the removal of atmospheric carbon through rates of input via background volcanic processes and the rates of removal via weathering of silicates and subsequent burial of marine carbonate sediments (Walker et al., 1981; Berner and Kothavala, 2001; Berner and Caldeira, 1997; Zeebe, 2012b; Uchikawa and Zeebe, 2008). This balance predicts that the very slow changes in atmospheric carbon should scale with the rate of emissions, steady state balance is thought to be achieved on timescales >100kyr. Representing the weathering rate by

$$F_{si} = F_{si}^0 (p\text{CO}_2)^{n_{si}} \quad (1)$$

where F_{si}^0 is the constant background weathering rate and in addition, should exhibit a strong sensitivity to the functional form of silicate weathering, that is, its dependence on temperature and atmospheric $p\text{CO}_2$ content (Walker et al., 1981). This particular balance has been widely used in paleoclimate studies because it offers a concise interpretation of past climate events in terms of changes in the rate of carbon emission. However, relatively little attention has been paid to questions of how well this balance applies to transient emissions with widely varying magnitudes and durations is the atmospheric partial pressure of carbon dioxide, this balance yields $p\text{CO}_2 \propto (E/D)^{1/n_{si}}$, where E is the total emission and D is the duration over which the carbon is emitted. In this limit, the climate is extremely sensitive to the strength of the weathering parameter, n_{si} .

The purpose of this paper is to examine whether a similar set of scaling laws exist for large emissions with timescales much shorter than millions of years. Given the variety of

timescales involved in the interactions between the different carbon reservoirs it is by no means certain that such scalings exist. We show that they do, but that their actual values depend on the basic state of the system. The scalings thus provide a way to quantify the stability of the carbon cycle through Earth history.

~~We are interested in~~ Our scalings characterize the response of the Earth system to emission events with sizes ranging from hundreds to tens of thousands petagrams of carbon (PgC) and durations ranging from one hundred years to one hundred thousand years. In principle this information could be generated using three-dimensional Earth System Models, as it has been for anthropogenic perturbations (Sarmiento et al., 1998; Matsumoto et al., 2004). However ~~because of their focus on short-term climate change~~, relatively few of the comprehensive Earth system models ~~have included~~ used to project century-scale climate change include interactions with the sediments (an exception being the Bergen Climate Center of Tjiputra et al., 2010). ~~Moreover, the~~ A number of Earth system models of intermediate complexity (e.g. GENIE-1 (Ridgwell et al., 2007)) do, however, include these interactions with the sedimentary reservoir. Both the comprehensive and intermediate complexity Earth System Models require very long run times (on the order of hundreds of thousands of years) ~~that are necessary in order~~ to capture the entire history of a perturbation ~~represent~~. This represents a significant computational burden ~~for these models~~, making it difficult to ~~run enough cases rapidly explore the variety of emission totals and time-scales needed~~ to generate scaling laws. Accordingly, in this study we adopt a more streamlined approach, using a simplified Earth system model suitable for representing the carbon cycle on hundred thousand year timescales and focusing our attention on perturbations to globally-averaged properties rather than local effects.

In this paper we ~~derive~~ find scaling laws that link perturbations of Earth system variables to atmospheric CO₂ emission size and duration. We use the LOSCAR carbon cycling model (Zeebe et al., 2009; Zeebe, 2012b) to determine quantitative relationships between the magnitude of perturbations to Earth system variables such as atmospheric CO₂, ocean acidity and alkalinity, and carbon isotope anomalies and idealized transient CO₂ emissions that differ only in terms of their duration and total size. Analyzing the system response

to such CO₂ emissions ranging in total size from ~~100~~50 to 50 000 PgC and durations from ~~100~~50 years to 100 kyr, we find that most Earth system variable perturbations can be scaled using power law formulas, ~~but with exponents that differ substantially from what is expected on the basis of simplified equilibrium considerations.~~ As these power laws depend on the physical setup they represent a compact way of characterizing how different climates respond to large transient perturbations.

4 Previous work

~~LOSCAR has been employed to investigate a range of problems for both paleo and modern climate applications. It has specifically been used to study the impacts of large transient emissions such as those found during the Paleocene-Eocene Thermal Maximum (PETM), as well as modern Anthropogenic emissions.~~

~~For paleoclimate applications LOSCAR has been used to constrain the transient emission needed to produce the observed Earth system responses found during the PETM (Zeebe et al., 2009), and more generally, to investigate the response of atmospheric and ocean chemistry to carbon perturbation throughout the Cenozoic with different seawater chemistry and bathymetry (Stuecker and Zeebe, 2010). Particular applications include constraining the range of the pH effects on carbon and oxygen isotopes in organisms during the PETM perturbation (Uchikawa and Zeebe, 2010), to investigate the effects of weathering on the inventory of the oceans during the PETM (Komar and Zeebe, 2011), to infer changes in ocean carbonate chemistry using the Holocene atmospheric record (Zeebe, 2012a), and to investigate different processes that potentially generated large scale fluctuations in the calcite compensation depth (CCD) in the middle to late Eocene (Pälike et al., 2012). Other applications include analysis of perturbations to the carbon cycle during the Middle Eocene Climatic Optimum (MECO) (Sluijs et al., 2013), and study of effects of slow methane release during the early Paleogene (62–48) (Komar et al., 2013).~~

For the modern climate applications LOSCAR has been used to show how decrease in ocean pH is sensitive to carbon release time, specifically for possible future anthropogenic release scenarios (Zeebe et al., 2008), to determine whether enhanced weathering feedback can mitigate future rise (Uchikawa and Zeebe, 2008), to study effects of increasing ocean alkalinity as a means to mitigate ocean acidification and moderate atmospheric p (Paquay and Zeebe, 2013), and to compare modern perturbations with those inferred during the PETM, to assess the long-term legacy of massive carbon inputs (Zeebe and Zachos, 2013).

4 Methods

Figure 1 is a schematic illustrating the type of forcing considered in this study and the nature of the Earth system response. Figure 1a shows a CO_2 emission event with a symmetric, triangular-shaped emission rate history superimposed on a steady background emission rate, R_o . This background emission represents the steady-state injection of carbon into the atmosphere from volcanic and metamorphic sources. The transient emission starts at time t_o and ends at time $t_o + D$, so that D is its duration. The total emission in the event, E , is related to its duration and peak emission rate, R_{peak} , by $E = D\Delta R/2$, where $\Delta R = R_{\text{peak}} - R_o$. By virtue of the assumption of symmetry, R_{peak} occurs at time $t_o + D/2$. Figure 1b shows the response of a typical system variable, V . The system variable changes with time from its initial value V_o , to its peak value V_{peak} , then relaxes back toward V_o . We define the peak system response as $\Delta V = |V_{\text{peak}} - V_o|$, the absolute value being necessary in this definition because some system variables respond with negative perturbations. In this study we seek mathematical relationships connecting ΔV to D and E .

LOSCAR is a box model designed for these objectives. ~~As noted above, it has been applied to a number of events in the paleoclimate record.~~ It has been employed to investigate a range of problems for both paleo and modern climate applications. LOSCAR allows for easy switching between modern and Paleocene/Eocene ocean configurations. It has specifically been used to study the impacts of large transient emissions such

as those found during the Paleocene-Eocene Thermal Maximum (PETM), as well as modern anthropogenic emissions. For the modern Earth, LOSCAR components include the atmosphere and a three-layer representation of the ~~major ocean basins~~ (Atlantic, Indian, and Pacific) ~~(and Tethys for the paleo version)~~ ocean basins, coupled to a marine sediment component (Zeebe, 2012b). The marine sediment component consists of sediment boxes in each of the major ocean basins arranged as functions of depth. The ocean component includes a representation of the mean overturning circulation as well as mixing. Biological cycling is parameterized by restoring surface nutrients to fixed values. In the simulations described here, the circulation and target surface nutrients are kept independent of climate change, so that we focus solely on contrasting surface weathering and sedimentary responses. Biogeochemical cycling in LOSCAR also includes calcium carbonate (CaCO_3) dissolution, weathering and burial, silicate weathering and burial, calcite compensation, plus carbon fluxes between the sediments, the ocean basins, and the atmosphere. Carbonate dissolution is limited by including variable sediment porosity. In addition, LOSCAR includes a high-latitude surface ocean box without sediments but otherwise coupled to the other ocean basins through circulation and mixing. Table 3 lists the important model variables, including their notation and dimensional units.

For the modern climate applications LOSCAR has been used to show how decrease in ocean pH is sensitive to carbon release time, specifically for possible future anthropogenic release scenarios (Zeebe et al., 2008), to determine whether enhanced weathering feedback can mitigate future $p\text{CO}_2$ rise (Uchikawa and Zeebe, 2008), to study effects of increasing ocean alkalinity as a means to mitigate ocean acidification and moderate atmospheric $p\text{CO}_2$ (Paquay and Zeebe, 2013), and to compare modern perturbations with those inferred during the PETM, to assess the long-term legacy of massive carbon inputs (Zeebe and Zachos, 2013).

For paleoclimate applications LOSCAR has been used to constrain the transient emission needed to produce the observed Earth system responses found during the PETM (Zeebe et al., 2009), and more generally, to investigate the response of atmospheric CO_2 and ocean chemistry to carbon perturbations throughout the Cenozoic with different

seawater chemistry and bathymetry (Stuecker and Zeebe, 2010). Particular applications include constraining the range of the pH effects on carbon and oxygen isotopes in organisms during the PETM perturbation (Uchikawa and Zeebe, 2010), to investigate the effects of weathering on the $[Ca^{2+}]$ inventory of the oceans during the PETM (Komar and Zeebe, 2011), to infer changes in ocean carbonate chemistry using the Holocene atmospheric CO_2 record (Zeebe, 2012a), and to investigate different processes that potentially generated large scale fluctuations in the calcite compensation depth (CCD) in the middle to late Eocene (Pälike et al., 2012). Other applications include analysis of perturbations to the carbon cycle during the Middle Eocene Climatic Optimum (MECO) (Sluijs et al., 2013), and study of effects of slow methane release during the early Paleogene (62–48 Ma) (Komar et al., 2013).

5 Case study results

Figures 2–7 show the LOSCAR response to an emission event idealized emission event of the type shown in Fig. 1 with size $E = 1000$ PgC and duration $D = 5$ kyr of the type illustrated in Fig. 1. This particular example was initialized in the modern LOSCAR configuration using steady-state preindustrial conditions with an atmospheric $pCO_2 = 280$ ppmv corresponding to a total atmosphere carbon content, $TC_{atm} = 616$ PgC. The initial total carbon content of the global oceans was $TC_{ocn} = 35852$ PgC and the initial global ocean total alkalinity (TA) was $TA = 3.1377 \times 10^{18}$ mol. The emission event began 100 years after startup and its duration is indicated by shading in the figures. This calculation, like all of the others in this study, spans 5 Myr in order to ensure that final equilibrium steady state conditions are reached.

The resulting changes in total ocean and atmosphere carbon, TC_{ocn} and TC_{atm} respectively, are shown in Fig. 2a as functions of time in log units. The atmosphere peak perturbation occurs about 3744 about 3700 years after emission onset, whereas the ocean perturbation peaks about 26 440 400 years after emission onset. There is an inflection point in the atmosphere response nearly corresponds corresponding to the peak ocean

response and is an example of the ~~carbon tail~~ phenomenon. This particular carbon tail. The leveling out of the atmospheric perturbation is due to ocean-sediment interactions and differs from the carbon tail described by Archer et al. (2009), which is controlled primarily by silicate weathering fluxes.

5 Figure 2b shows the corresponding rates of change of TC_{ocn} and TC_{atm} . The curves labeled Atm and Ocn are the time derivatives from Fig. 2a, and the curve labeled Total is their sum. Also shown in Fig. 2b is the adjusted total, the difference between the total rate of change in the atmosphere + ocean and $R - R_o$. The adjusted total, which corresponds to the rate at which additional carbon is added to the ocean-atmosphere system through
10 the reactive processes of weathering, CaCO_3 dissolution, and calcite compensation, peaks at 0.16 PgC yr^{-1} and is positive for about the first 10 kyr after emission onset. This behavior demonstrates how these reactive processes amplify the ~~carbon perturbation~~ total carbon perturbation to the system coming directly from an emission event. The logarithmic time scale (necessary to capture both the fast rise and slow fall-off of the carbon perturbation) obscures the important fact that these reactive processes play a quantitatively significant
15 role, accounting for a significant fraction of the large rise in oceanic carbon that occurs after the atmospheric peak.

Because additional carbon enters the system through reactive processes of weathering and marine sediment dissolution and leaves the system through deposition, the total carbon
20 perturbation at any given time generally does not equal the total emission up to that time. To quantify this effect we define gain factors, which are ratios of total carbon perturbation to total emission E measured at time t . For the atmosphere and ocean these are:

$$G_{\text{atm}}(t) = \frac{TC_{\text{atm}}(t) - TC_{\text{atm}}(t_o)}{E(t)} \quad (2)$$

$$G_{\text{ocn}}(t) = \frac{TC_{\text{ocn}}(t) - TC_{\text{ocn}}(t_o)}{E(t)}. \quad (3)$$

We also define gain factors for the ocean–atmosphere system as

$$G_{\text{sys}}^+(t) = G_{\text{atm}}(t) + G_{\text{ocn}}(t) \quad (4)$$

$$G_{\text{sys}}^-(t) = G_{\text{atm}}(t) - G_{\text{ocn}}(t). \quad (5)$$

According to these definitions, G_{sys}^+ is the gain of the system as a whole. G_{sys}^- gives information on the time dependent partitioning of carbon between the atmosphere and ocean reservoirs. After emissions onset a value of $0 < G_{\text{sys}}^- < 1$ indicate that the atmospheric reservoir contains relatively more of the perturbation. The zero crossing of G_{sys}^- indicates the time when the relative system response is equivalent in the atmosphere and ocean reservoirs. Values of $G_{\text{sys}}^- < -1$ indicate that the system has amplified the perturbation with the majority of the additional carbon being found in the ocean reservoir.

Figure 3 shows these gain factors as a function of time for the emission event from Fig. 2. G_{atm} decreases monotonically over the duration of the emission; the small residual in G_{atm} following the emission is an example of the classical carbon tail shows the long tail of the lifetime of the carbon in the atmosphere (Archer et al., 2009). In contrast, G_{ocn} rises during the emission and continues to increase until it peaks at 1.68, about 26 438 450 years after emission onset, then decreases to unity after 378 about 380 850 000 years, and finally returns to zero. Similarly, G_{sys}^+ generally rises during the emission, peaking at a value of 1.76 around 25 000 years after emission onset, then decreasing to unity after around 408 260 000 years. G_{sys}^- is almost a mirror image of G_{ocn} , indicating that the sediments are contributing more carbon to the ocean than to the atmosphere during this time.

The response of the ocean layers is shown in Fig. 4. Figure 4a shows the time variations in pH in each ocean layer as well as the global ocean total alkalinity. Note that pH variations lead TA in time; first pH drops and TA begins to rise in response, then pH recovers and later TA recovers. The minima in the ocean surface, intermediate, and deep layer pH occur 3618, 3797 about 3600, 3800, and 4600 years respectively, after emission onset. In contrast, the maximum TA occurs about 30 455 500 years after emission onset (by which time the the pH is almost fully recovered) and the TA does not fully recover for more than one million years.

Effects of the emission event on Atlantic Ocean sediments are shown in Fig. 4b. The deeper sediments respond earlier and take longer to recover from the perturbation compared to the shallower sediments. In addition, the sediments at 5000 and 5500 m depths do not recover monotonically, but instead overshoot their initial state, becoming relatively enriched in carbonate for tens of thousands of years. This transient enrichment process has been explained ~~by Zeebe (2012b)~~ in Zachos et al. (2005) as a direct consequence of the weathering feedback, where the enhanced weathering, due to elevated $p\text{CO}_2$, increases the ocean saturation state and deepens the CCD to balance the riverine and burial fluxes.

Figure 4c shows the ~~unweighted volume-weighted~~ average temperature perturbations, ~~which contrast with TA by recovering on timescales of order thousands of years, rather than tens of thousands. Peak temperatures~~. Peak temperature perturbations occur between ~~3743 and 4814~~ 3700 and 4900 years after emission onset. Although the atmospheric temperature ~~mostly recovers after a couple of thousands of years, there remains a small anomaly remains elevated~~ for longer periods due to coupling with $p\text{CO}_2$ in the atmosphere, which ~~as discussed before~~ has an extended carbon tail lifetime for up to millions of years, depending on the strength of prescribed weathering feedbacks (Archer et al., 2009; Komar and Zeebe, 2011).

Figure 5 shows the sediment carbonate content for each ocean basin as a function of depth, with colors indicating the starting, maximum, and minimum values that were recorded in each depth box. The deep boxes are most perturbed because they are directly affected by movement of the CCD. In addition, sediments in the deep Atlantic are perturbed more than those in the Pacific or Indian basins because the CCD is deeper in the Atlantic. Far more carbon enrichment occurs in the Atlantic, for example, the 5000 m box starts at 22 % carbonate and during the run increases to close to 50 %.

Figure 6 shows the time derivative of global TA for the aforementioned case. The red curve accounts for the known contributions of TA from weathering feedbacks and therefore depicts the alkalinity flux that is due to dissolution, and subsequent burial of marine carbonates. Where the red curve is positive it denotes a net dissolution of carbonates;

where it is negative it denotes a net burial of carbonates. The peak fluxes occur ~~3618~~about 3600 years after emission onset, simultaneous with the peak in the average surface pH. Figure 6 shows the dominance of sediment processes in determining the total alkalinity. In this simulation $\approx 80\%$ of the maximum flux of alkalinity to the ocean is due to dissolution of sediments, which helps to explain the relatively minor role played by weathering in determining the peak atmospheric carbon dioxide.

5 Figure 7 shows the $\delta^{13}\text{C}$ isotope signature for the atmosphere and ocean boxes as a function of time for the case of $E = 1000 \text{ PgC}$ and $D = 5 \text{ kyr}$. The signatures of the surface, intermediate, and deep lines were defined by calculating the ~~unweighted~~volume-weighted average across basins. The atmosphere and surface ocean perturbations are felt before the deeper ocean boxes. The peak surface signature is ~~4018~~around
 10 4000 years after emission onset. The peak deep signature occurs ~~5337~~about 5400 years after emission onset, more than 1300 years after it peaks at the surface.

6 Power law scalings

Table 1 compares two cases which differ in D and E but share the same ΔR . If the system response was linear~~we would expect~~, the perturbations in these two cases ~~to~~would be in proportion to E , i.e., differ in their response by $20\times$. However, Table 1 shows that none of these variables are in the proportion of $20 : 1$. ~~Alternatively, if the response were nonlinear but depended~~For a nonlinear response that depends only on ΔR , ~~we would expect these variables to~~these variables would be in constant proportion other than $20 : 1$. This is not the case either. Accordingly, a more general formulation is needed to systematize these results.

20 A power law relationship between the the peak change in a system variable ΔV and the total magnitude and duration of the emission event shown in Fig. 1 can be written as

$$\Delta V = \gamma D^\alpha E^\beta \quad (6)$$

where the coefficient γ and the exponents α and β assume different values for each system variable. Alternatively, Eq. (6) can be written in terms of emission rate using $\Delta R = 2E/D$,

$$\Delta V = 2^{-\beta} \gamma D^{\alpha+\beta} \Delta R^{\beta} = 2^{\alpha} \gamma E^{\alpha+\beta} \Delta R^{-\alpha} \quad (7)$$

If the peak change in ΔV depends only on the peak emissions rate, ΔR , ~~as suggested for the atmosphere by the simple equilibrium balance between volcanic emission and silicate weathering fluxes, then we expect~~ then $\alpha = -\beta$ in Eqs. (6) and (7). Other simple balances are possible. For example, it may be that the peak values depend on the actual time varying emissions rate $R'(t) = R(t) - R_o$. ~~In LOSGAR the evolution of atmospheric is determined by~~

$$\frac{d}{dt}(\text{TC}_{\text{atm}}) = F_{\text{vc}} + F_{\text{gas}} - F_{\text{cc}} - 2F_{\text{si}} + R'$$

~~where F_{vc} is the flux due to volcanic degassing, F_{gas} is the flux due to air-sea gas exchanges, F_{cc} and F_{si} are the carbonate and silicate weathering fluxes respectively, and R' is the flux from emissions. The weathering fluxes F_{cc} and F_{si} are parameterized in LOSGAR in the following form (Zeebe, 2012b; Walker et al., 1981; Berner et al., 1983; Walker and Kasting, 1992):~~

$$F_{\text{cc}} = F_{\text{cc}}^0 \left(\frac{p\text{CO}_2}{p\text{CO}_2^0} \right)^{\text{ncc}}$$

$$F_{\text{si}} = F_{\text{si}}^0 \left(\frac{p\text{CO}_2}{p\text{CO}_2^0} \right)^{\text{nsi}}$$

~~Where the superscript 0 refers to the long-term steady state, and ncc and nsi are constant exponents. As described in Zeebe (2012b) the long-term steady state of p in LOSGAR is reached via removal of atmospheric carbon through weathering of silicates and subsequent burial as marine carbonate sediments. Following emissions onset, Eq. (8) reduces approximately to a long-term flux balance in which $F_{\text{vc}} = F_{\text{si}}$.~~

$$F_{\text{si}} \propto R'$$

since

$$F_{\text{si}} \propto (p\text{CO}_2)^{\text{nsi}}$$

Equation (8) yields

$$p\text{CO}_2 \propto (R')^{\frac{1}{\text{nsi}}}$$

which suggests that the change in atmospheric carbon should scale with R' and exhibit a $1/\text{nsi}$ sensitivity. Because nsi is usually assumed to be relatively small, a very strong sensitivity of climate to emissions is implied by Eq. (8).

Our scaling analysis considers only peak values of the perturbed variables. To determine global ocean carbon content we multiplied the dissolved inorganic carbon (DIC) concentrations in each of the ocean boxes by their prescribed volumes to obtain the total mass of carbon in each box. We then summed over all the ocean boxes to define the variable TC_{ocn} . We used this same procedure to determine the global ocean total alkalinity. For analysis of temperature, $\delta^{13}\text{C}$, and pH we calculated the unweighted volume-weighted averages for the surface, intermediate and deep ocean boxes, respectively. Once peak variables were obtained we then performed a regression analysis against D and E for each system variable.

Results of this procedure for TC_{atm} , TC_{ocn} , and TA are shown in Figs. 8–10. Figures 8a, 9a, and 10a show the unscaled peak changes of these variables vs. E for different D values. $\Delta\text{TC}_{\text{atm}}$ has a distinct dependence on D , whereas $\Delta\text{TC}_{\text{ocn}}$ and ΔTA have virtually none. Figures 8b, 9b, and 10b show the peak changes scaled according to Eq. (6). The peak changes in Figs. 9b and 10b vary linearly with emissions size E , and accordingly the scaled results collapse to a power law fit with negligible deviation. In Fig. 8b, however, the power law behavior of $\Delta\text{TC}_{\text{atm}}$ fit is limited to the range $10^2 < E < 10^4$ PgC. The deviation at the upper end of this range is due to the fact that the carbonate sediments cannot be dissolved without limit; at some point the accessible carbon reservoir in the sediments becomes exhausted. In addition, the conditions for chemical equilibrium used in LOSGAR lose validity at high

ocean temperatures, so the scaling laws on which they are based lose validity there as well.

Tables 4–6 give the results of our power law scalings for the Modern LOSCAR configuration in terms of best-fitting values for the exponents α and β , the preexponential coefficients γ , and the R value of the fit. Although $\alpha < 0$ and $\beta > 0$ for all variables ~~except the GGD in the Indian Ocean~~, as expected, large differences in some of the exponents are evident. For example, TC_{atm} and TC_{oce} have very different dependences on duration D , with the atmosphere exponent having a value of ~~$\alpha = -0.32$~~ $\alpha = -0.289$ and the ocean exponent having a value of ~~$\alpha = -0.003$~~ $\alpha = -0.0035$. These variables also have different β -dependences, with the atmosphere exponent having a value of ~~$\beta = 1.22$~~ $\beta = 1.174$ and the ocean having a relatively weaker exponent value of ~~$\beta = 0.098$~~ $\beta = 0.982$. Note, however, that $\alpha + \beta \simeq 1$ for both of these, as well as for TA. Ocean and atmosphere temperatures generally have smaller β values and $\alpha + \beta$ in the range 0.6–0.8.

Scalings for the $\delta^{13}\text{C}$ variables in the atmosphere and in the upper and intermediate ocean boxes show dependence on duration, while the deep ocean box shows negligible dependence. This result suggests that by using the isotopic signatures from organisms from different depths that were deposited at the same time, one could explicitly solve for the E and D that produced that particular isotopic excursion. In general, the duration dependence of ocean variables weakens going from surface downward.

7 Power law scalings for the Paleo/Eocene

Following the same procedures in the previous section, we conducted a scaling analysis for the Paleocene/Eocene version of LOSCAR, which has different boundary and initial conditions than the modern version. Notable differences include the addition of the Tethys ocean basin, higher ocean temperatures, and different seawater chemistry, steady-state weathering fluxes and ocean circulation patterns. The detailed descriptions of this model configuration can be found in Zeebe (2012b).

These simulations were initialized using steady-state pre-PETM conditions with an atmospheric $p\text{CO}_2 = 1000$ ppmv corresponding to a total atmosphere carbon content, $\text{TC}_{\text{atm}} = 2200$ PgC. The initial total carbon content of the global oceans was $\text{TC}_{\text{ocn}} = 34196$ PgC and the initial global ocean total alkalinity (TA) was $\text{TA} = 2.7895 \times 10^{18}$ mol. The idealized emission events began 100 years after startup. The run lengths, like in the modern configuration, also spanned 5 Myr in order to ensure that final steady state conditions were reached. Tables 7–9 give the results of our power law scalings for this configuration.

Comparison of the scalings show that the responses to transient perturbations are qualitatively similar across the two climates. Figures 13–15 show the correlations of peak perturbations in the two configurations. For most emission events the correlation is high; however, there are systematic deviations for some variables. For example, the paleo ocean systematically takes up less carbon than the modern ocean (Fig. 13b) leaving more in the atmosphere (Fig. 13a). This is likely to be due to higher paleo temperatures and lower alkalinities resulting in weaker ocean buffering capacity. The changes in pH, however, are systematically larger in the modern ocean compared to the paleo (Fig. 14a). The relatively small changes in carbonate chemistry are unlikely to explain the systematics (doubling $p\text{CO}_2$ with the paleo surface temperature of 25°C and an alkalinity of $2000 \mu\text{M}$ gives almost the same change in pH as a modern temperature of 20°C and an alkalinity of $2300 \mu\text{M}$). The differences in pH are possibly due to differences in the carbonate weathering feedbacks or because the ocean circulation is stronger in the paleo version. Carbon-13 anomalies tend to be smaller at the surface in the paleo version, but the deep anomalies are essentially identical in both (Fig. 15).

8 Scaling law exponent sensitivity to variations in weathering feedbacks

Examples of system variable sensitivity to n_{si} and n_{cc} , within [LOSCAR](#), have been explored in previous studies (Uchikawa and Zeebe, 2008; Komar and Zeebe, 2011), but the relative range of these values studied was restricted by only considering enhanced feedbacks due

to nominal values of these parameters (Zeebe, 2012b). Here we consider a broader range of these values [in the modern LOSCAR configuration](#) to determine α and β sensitivity to large variations in the strength of these feedbacks. Table 2 shows the cases considered.

Figure 11 shows the resulting α and β values for the cases in Table 2 for the peak changes in TC_{atm} , TC_{ocn} , and TA. Figure 11a shows that as ncc increases while holding nsi at the default value, the resulting α values for TC_{atm} become more negative. Increasing nsi , while holding ncc at the default value, also results in more negative α values. Figure 11b shows that as ncc increases while holding nsi at the default value, the resulting β values for TC_{atm} monotonically decrease. Increasing nsi , while holding ncc at the default value, also results in smaller β values. Figure 11c shows that as ncc increases while holding nsi at the default value, the resulting α values for TC_{ocn} decrease negligibly. Increasing nsi , while holding ncc at the default value, also results in negligible changes in α values. Figure 11d shows that as ncc increases while holding nsi at the default value, the resulting β values for TC_{ocn} monotonically increase. Increasing nsi , while holding ncc at the default value, produces monotonically decreasing β values. Figure 11e shows that increasing ncc , while holding nsi at the default value, yields negligible changes in α values for TA. Increasing nsi , while holding ncc at the default value, also results in negligible changes in the α values. Figure 11f shows that as ncc increases while holding nsi at the default value, the resulting β values for TA monotonically increase; similar to the behavior in Fig. 11d. Also increasing nsi , while holding ncc at the default value, yields smaller β values like those in Fig. 11d. In summary Fig. 11 shows that β values are relatively more sensitive to changes in weathering strengths, ~~but that sensitivity is much weaker than would be anticipated from the two term atmospheric balance.~~

9 Discussion

The results presented in the previous section raise a number of important questions. In this section we further examine these, in particular – (1) Why is the dependence on weathering

so weak? (2) What controls the maximum in CO_2 ? And (3) What does this imply about additional feedbacks in the system?

Considerable insight can be gained into how the maximum $p\text{CO}_2$ is set by noting that the bicarbonate ion concentration at equilibrium is given by

$$[\text{HCO}_3^-] = \frac{k_H k_1 p\text{CO}_2}{[\text{H}^+]} \frac{k_H k_1 p\text{CO}_2}{[\text{H}^+]}. \quad (8)$$

where k_H is the Henry's law coefficient and k_1 is a dissociation coefficient, and $[\text{H}^+]$ is the hydrogen ion concentration. Similarly, the equilibrium carbonate ion concentration is given by

$$[\text{CO}_3^{2-}] = \frac{k_H k_1 k_2 p\text{CO}_2}{[\text{H}^+]^2}. \quad (9)$$

Then we can solve for the $p\text{CO}_2$ from Eqs. (8) and (9)

$$p\text{CO}_2 = \frac{k_2}{k_H k_1} \frac{[\text{HCO}_3^-]^2}{[\text{CO}_3^{2-}]}. \quad (10)$$

Letting TDIC denote the total

Letting DIC be the dissolved inorganic carbon and TA the total alkalinity, we can approximate Eq. (10) as in Sarmiento and Gruber (2006) by

$$p\text{CO}_2 \approx \frac{k_2}{k_H k_1} \frac{(2\text{TDIC} - \text{TA})^2}{\text{TA} - \text{TDIC}}$$

This approximation is only valid when the aqueous ALK the carbonate alkalinity and $C = k_H p\text{CO}_2$, the aqueous $p\text{CO}_2$ is small in comparison with the carbonate ion concentration, as it is in the modern ocean. However, the additional mathematical complexity that results from adding aqueous, we find that

$$p\text{CO}_2 \approx \frac{k_H k_1}{k_2} \frac{(2 \text{DIC} - \text{ALK} + C)^2}{(\text{ALK} - \text{DIC})} \quad (11)$$

5 When $p\text{CO}_2$ to Eq.(11), (converting it to a quadratic equation in is at a maximum $\partial C/\partial t$ is likewise zero so that we can find a relationship between $\partial \text{DIC}/\partial t$ and $\partial \text{ALK}/\partial t$. Taking the derivative with respect to time at the maximum $p\text{CO}_2$), largely adds complexity to the solutions developed below without adding much in the way of physical content.

$$\frac{2(2 \text{ DIC} - \text{ ALK} + \text{ C})}{(\text{ ALK} - \text{ DIC})} \left(2 \frac{\partial \text{ DIC}}{\partial t} - \frac{\partial \text{ ALK}}{\partial t} \right) - \frac{(2 \text{ DIC} - \text{ ALK} + \text{ C})^2}{(\text{ ALK} - \text{ DIC})^2} \left(\frac{\partial \text{ ALK}}{\partial t} - \frac{\partial \text{ DIC}}{\partial t} \right) = 0 \quad (12)$$

10 Which can be solved to give us

$$\frac{\partial \text{ ALK}}{\partial t} = \frac{3 \text{ ALK} - 2 \text{ DIC} + 2 \text{ C}}{\text{ ALK}} \frac{\partial \text{ DIC}}{\partial t} \quad (13)$$

Which can also be rewritten as

$$\frac{\partial \text{ ALK}}{\partial t} = [\text{ HCO}_3^-] + 4[\text{ CO}_3^{2-}] [\text{ HCO}_3^-] + 2[\text{ CO}_3^{2-}] \frac{\partial \text{ DIC}}{\partial t} \quad (14)$$

15 So that the maximum in $p\text{CO}_2$ is reached when the alkalinity change is a little higher than the DIC change. Since

$$\frac{[\text{ HCO}_3^-]}{[\text{ CO}_3^{2-}]} = k_2 / [\text{ H}^+] \quad (15)$$

20 we can rewrite this as

$$\frac{\partial \text{ ALK}/\partial t}{\partial \text{ DIC}/\partial t} = \theta = 1 + 4 \frac{k_2}{[\text{ H}^+]} \frac{[\text{ H}^+]}{1 + 2 k_2 / [\text{ H}^+]} \quad (16)$$

Within this approximation there ~~There~~ are two possible ways for $\partial p\text{CO}_2/\partial t$ to equal zero in Eq. (11). The first is the equilibrium regime where ~~$\partial\text{TA}/\partial t = \partial\text{TDIC}/\partial t = 0$~~ the emissions occur over very long time scales and the surface changes in TDIC and ALK mirror the ocean-average changes. This is the regime in which we would expect to find a strong dependence on weathering parameters. However, as can be seen from looking at Fig. 12, our transient simulations are characterized by a *dynamic* balance where both TDIC and TA are changing. ~~Setting the time derivative of Eq. (11) to zero and rearranging gives-~~

$$\frac{\partial\text{TDIC}}{\partial t} = \left(\frac{\text{TA}}{3\text{TDIC} - 2\text{TA}} \right) \frac{\partial\text{TA}}{\partial t}$$

Given that the TDIC and TA are quite similar in size, this implies that a dynamic equilibrium can be achieved when-

$$\frac{\partial\text{TA}/\partial t}{\partial\text{TDIC}/\partial t} = \theta \approx 1$$

This dynamic balance means that it is the growth of alkalinity within the ocean that brings atmospheric $p\text{CO}_2$ into balance. Examining θ at the time of maximum $p\text{CO}_2$ (Fig. 12a) shows that the two terms are approximately the same for all the runs with durations of ~~5000, 25 10 000, 50 000~~ 5000, 25 10 000, 50 000 and 100 000 years. ~~This makes sense because the uptake of carbon in the short duration cases is determined by the~~ For surface temperatures of around 20°C, $k_2 \approx 10^{-9}$ so that the ratio between alkalinity and DIC change is around about 1.2 at low emissions. As the pH increases for longer time scales this ratio drops towards 1.

~~For short durations, by contrast, the peak is found when θ is very small. Rather than carbonate reactions being important, what matters is the~~ ability of the ocean circulation to move carbon away from the surface rather than by weathering feedbacks. Indeed, careful. Careful examination of these cases shows that the bulk of added carbon dioxide resides in the atmosphere. ~~However, as the duration of the emissions pulse becomes long in comparison with the overturning timescale of the oceans, the basic balance in Eq. (17) holds.~~

The relatively weak dependence of θ on total emissions obscures an interesting difference between short and long-duration pulses. For short-duration pulses, θ increases as the emissions increase. As more and more carbon is added to the system over short periods of time, more of it reacts with calcium carbonate, and increases ocean alkalinity. However, for the long-duration simulations, the dependence runs in the opposite direction, with higher emissions showing less compensation from alkalinity.

To first-order, a situation in which the growth rates in TDIC and TA are equal is what one would expect in a system without burial, where the additional carbon added to the atmosphere reacts with silicate rocks, and the additional alkalinity ends up accumulating in the ocean. Such a situation would also be expected to have a strong dependence on weathering parameters. However, in LOSCAR the dominant flux of alkalinity is often from the sediments to the ocean. This flux will grow not just because the deep ocean pH ~~increases~~decreases, but because more sediments are mobilized as this happens.

At intermediate durations the picture becomes much more complicated. There appears to be an optimal emission for maximizing interactions with the sediments. The reasons for this are unclear, but it is striking that the time scales involved are similar to the timescales for ocean overturning.

Note that the discretization of the deep ocean into a fixed number of boxes introduces some step-like behavior in the volume of sediments mobilized, which can be seen in Fig. 12b. The fact that less sediment is available for interaction as the lysocline shallows may explain part of why θ drops at high emission in Fig. 12b. In any case, we expect the sediment alkalinity flux to have a functional dependence on the perturbation DIC, which is linear or superlinear, implying that it has the potential to overwhelm the rather weak dependence on $p\text{CO}_2$ ~~prescribed generally used in Eqs. (8) and (8).~~

~~The importance of sediment interactions may explain why LOSCAR gives different results than other models~~Our results suggest future sensitivity studies. For example, ~~recent work by ? examines the carbon-13 isotope anomaly at the end of the Permian using the eGENIE model of Ridgwell and Hargreaves (2007). In that model an atmospheric perturbation of around 17500biogenic carbon with an isotope anomaly of -25is associated~~

with a carbon-13 anomaly of around 3‰ in shallow carbonates lasting about 60000. Our scaling would predict such an isotopic anomaly in surface waters would be associated with a total emission of only about 8000. Moreover, because much of this carbon interacts with sediments, only 1143 ends up in the atmosphere at the peak, causing a much smaller perturbation to global climate: What differences between the Paleocene/Eocene and modern world produce different scaling laws? Answers might be found in different ocean circulation patterns or different hypsometric distributions, which would then determine the amount of sediment available to react with CO₂.

Furthermore, our results suggest other important sensitivity studies. In particular, Additionally, the strong role played by the oceanic carbonate budget suggests additional feedbacks involving the biological pump. In the version of LOSCAR used here, the removal of organic material from the surface layer is primarily controlled by high-latitude nutrients and the ocean circulation, neither of which varies with CO₂ in our simulations. Additionally, the rain ratio of particulate inorganic carbon to organic carbon is held constant. All of these are likely to vary in the real world.

However, it should also be noted that a robust connection between these changes in the biological pump and climate remains uncertain. For example, today the deep ocean receives water injected from the North Atlantic, which in the modern world has relatively low surface nutrients, and the Southern Ocean, which has relatively high surface nutrients. As noted by Marinov et al. (2008), changes in the balance of deep waters formed from these regions can significantly alter the carbon stored by the biological pump in the deep ocean, so that a slowdown in circulation may produce either increased or decreased storage of carbon (with corresponding changes in deep ocean acidity). While one might expect the total level of vertical exchange to decrease as atmospheric carbon dioxide increases, it is much less clear how the balance between the two sources regions would change.

Similarly, there are open questions regarding the rain ratio. While it does seem likely that this value will be a function of carbon saturation state, it is not clear what the dependence should be. While some calcifying organisms like corals (Langdon et al., 2000) and pteropods (Fabry et al., 2008) tend to grow more slowly under higher levels of carbon

dioxide, other calcifying organisms such as coccolithophores may become more abundant (S. Rivero-Calle, personal communication, 2014).

[See supplementary material for an example of how the scaling laws, which are based on an idealized emission shape, may be used to estimate the peak perturbations from more realistic fossil fuel emission scenarios.](#)

Acknowledgements. This research has been supported by National Science Foundation Frontiers of Earth System Dynamics grant EAR-1 135 382. Special thanks to Richard Zeebe for making the LOSCAR code available.

References

Archer, D., Eby, M., Brovkin, V., Ridgwell, A., Cao, L., Mikolajewicz, U., and Caldeira, K., Matsumoto, K., Munhoven, G., Montenegro, A., and Tokos, K.: Atmospheric lifetime of fossil fuel carbon dioxide, *Annu. Rev. Earth Pl. Sc.*, 37, 117–134, 2009.

Berner, R. A. and Caldeira, K.: The need for mass balance and feedback in the geochemical carbon cycle, *Geology*, 25, 955–956, 1997.

Berner, R. A. and Kothavala, Z.: GEOCARB III: a revised model of atmospheric CO₂ over Phanerozoic time, *Am. J. Sci.*, 301, 182–204, 2001.

Berner, R. A., Lasaga, A. C., and Garrels, R. M.: The carbonate-silicate geochemical cycle and its effect on atmospheric carbon dioxide over the past 100 million years, *Am. J. Sci.*, 283, 641–683, 1983.

~~Gui, Y., Kump, L., and Ridgwell, A.: Initial assessment of the carbon emission rate and climatic consequences during the end-Permian mass extinction, *Palaeogeogr. Palaeoclimatol.*, 329, 128–136, 2013.~~

Fabry, V. J., Seibel, B. A., Feely, R. A., and Orr, J. C.: Impacts of ocean acidification on marine fauna and ecosystem processes, *ICES J. Mar. Sci.*, 65, 414–432, 2008.

Komar, N. and Zeebe, R. E.: Oceanic calcium changes from enhanced weathering during the Paleocene-Eocene Thermal Maximum: no effect on calcium-based proxies, *Paleoceanography*, 26, PA3211, doi:10.1029/2010PA001979, 2011.

Komar, N., Zeebe, R. E., and Dickens, G. R.: Understanding long-term carbon cycle trends: the late Paleocene through the early Eocene, *Paleoceanography*, 28, 650–662, 2013.

- Langdon, C., Takahashi, T., Sweeney, C., Chipman, D., and Atkinson, J.: Effect of calcium carbonate saturation on the calcification rate of an experimental coral reef, *Global Biogeochem. Cy.*, 14, 639–654, 2000.
- 30 Marinov, I., Gnanadesikan, A., Sarmiento, J. L., Toggweiler, J. R., Follows, M., and Mignone, B. K.: Impact of oceanic circulation on biological carbon storage in the ocean and atmospheric $p\text{CO}_2$, *Global Biogeochem. Cy.*, 22, GB3007, doi:10.1029/2007GB002958, 2008.
- Matsumoto, K., Sarmiento, J. L., Key, R. M., Aumont, O., Bullister, J. L., Caldeira, K., Campin, J.-M., Doney, S. C., Drange, H., Dutay, J.-C., Follows, M., Gao, Y., Gnanadesikan, A., Gruber, N., Ishida, A., Joos, F., Lindsay, K., Maier-Reimer, E., Marshall, J. C., Matear, R. J., Monfray, P., Mouchet, A., Najjar, R., Plattner, G.-K., Schlitzer, R., Slater, R., Swathi, P. S., Totterdell, I. J.,
- 5 Weirig, M.-F., Yamanaka, Y., Yool, A., and Orr, J. C.: Evaluation of ocean carbon cycle models with data-based metrics, *Geophys. Res. Lett.*, 31, L07303, doi:10.1029/2003GL018970, 2004.
- [McKay, D. J., Tyrrell, T., Wilson, P. A., and Foster, G. L.: Estimating the impact of the cryptic degassing of Large Igneous Provinces: A mid-Miocene case-study, *Earth and Planetary Science Letters*, 403, 254–262, 2014.](#)
- 10 Pälike, H., Lyle, M. W., Nishi, H., Raffi, I., Ridgwell, A., Gamage, K., Klaus, A., Acton, G., Anderson, L., Backman, J., Baldauf, J., Beltran, C., Bohaty, S. M., Bown, P., Busch, W., Channell, J. E. T., Chun, C. O. J., Delaney, M., Dewangan, P., Dunkley, J. T., Edgar, K. M., Evans, H., Fitch, P., Foster, G. L., Gussone, N., Hasegawa, H., Hathorne, E. C., Hayashi, H., Herrle, J. O., Holbourn, A., Hovan, S., Hyeong, K., Iijima, K., Ito, T., Kamikuri, S.-I., Kimoto, K., Kuroda, J., Leon-Rodriguez, L., Malinverno, A., Moore, T. C., Murphy, B. H., Murphy, D. P., Nakamura, H., Ogane, K., Ohneiser, C., Richter, C., Robinson, R., Rohling, E. J., Romero, O., Sawada, K., Scher, H., Schneider, L., Sluijs, A., Takata, H., Tian, J., Tsujimoto, A., Wade, B. S., Westerhold, T., Wilkens, R., Williams, T., Wilson, P. A., Yamamoto, Y., Yamamoto, S., Yamazaki, T., and Zeebe, R. E.: A Cenozoic record of the equatorial Pacific carbonate compensation depth,
- 15 *Nature*, 488, 609–614, 2012.
- Paquay, F. S. and Zeebe, R. E.: Assessing possible consequences of ocean liming on ocean pH, atmospheric CO_2 concentration and associated costs, *Int. J. Greenh. Gas Con.*, 17, 183–188, 2013.
- 20 Ridgwell, A. and Hargreaves, J.: Regulation of atmospheric CO_2 by deep-sea sediments in an Earth System Model, *Global Biogeochem. Cy.*, 21, GB2008, doi::10.1029/2006GB002764, 2007.

Ridgwell, A., Hargreaves, J. C., Edwards, N. R., Annan, J. D., Lenton, T. M., Marsh, R., Yool, A., and Watson, A.: Marine geochemical data assimilation in an efficient Earth System Model of global biogeochemical cycling, *Biogeosciences*, 4, 87–104, doi:10.5194/bg-4-87-2007, 2007.

Sarmiento, J. L. and Gruber, N.: *Ocean Biogeochemical Dynamics*, Princeton University Press, Princeton, NJ, 2006.

Sarmiento, J. L., Hughes, T. M. C., and Stouffer, R. J.: Simulated response of the ocean carbon cycle to anthropogenic climate warming, *Nature*, 393, 245–249, 1998.

Sluijs, A., Zeebe, R. E., Bijl, P. K., and Bohaty, S. M.: A middle Eocene carbon cycle conundrum, *Nat. Geosci.*, 6, 429–434, 2013.

Stuecker, M. F. and Zeebe, R. E.: Ocean chemistry and atmospheric CO₂ sensitivity to carbon perturbations throughout the Cenozoic, *Geophys. Res. Lett.*, 37, L03609, doi:10.1029/2009GL041436, 2010.

5 Tjiputra, J. F., Assmann, K., Bentsen, M., Bethke, I., Otterå, O. H., Sturm, C., and Heinze, C.: Bergen earth system model (BCM-C): model description and regional climate-carbon cycle feedbacks assessment, *Geosci. Model Dev.*, 3, 123–141, doi:10.5194/gmd-3-123-2010, 2010.

Uchikawa, J. and Zeebe, R. E.: Influence of terrestrial weathering on ocean acidification and the next glacial inception, *Geophys. Res. Lett.*, 35, L23608, doi:10.1029/2008GL035963, 2008.

10 Uchikawa, J. and Zeebe, R. E.: Examining possible effects of seawater pH decline on foraminiferal stable isotopes during the Paleocene-Eocene Thermal Maximum, *Paleoceanography*, 25, PA2216, doi:10.1029/2009PA001864, 2010.

Walker, J. C. G. and Kasting, J. F.: Effects of fuel and forest conservation on future levels of atmospheric carbon dioxide, *Palaeogeography, Palaeoclimatology, Paleocology, Global Planet. Change*, 97, 151–189, 1992.

15 Walker, J. C. G., Hays, P. B., and Kasting, J. F.: A negative feedback mechanism for the long-term stabilization of Earth's surface temperature, *J. Geophys. Res.*, 86, 9776–9782, 1981.

Zachos, J. C., Röhl, U., Schellenberg, S., Sluijs, S., Hodell, D. A., Kelly, D. C., Thomas, E., Nicolo, M., Raffi, I., Lourens, L. J., McCarren, H., and Kroon, D.: Rapid Acidification of the Ocean During the Paleocene-Eocene Thermal Maximum, *Science* 10 June 2005: 308 (5728), 1611–1615. [DOI:10.1126/science.1109004]

20 Zeebe, R. E.: History of seawater carbonate chemistry, atmospheric CO₂, and ocean acidification, *Annu. Rev. Earth Pl. Sc.*, 40, 141–165, 2012a.

1015 Zeebe, R. E.: LOSCAR: Long-term Ocean-atmosphere-Sediment CARbon cycle Reservoir Model v2.0.4, *Geosci. Model Dev.*, 5, 149–166, doi:10.5194/gmd-5-149-2012, 2012b.

1020 Zeebe, R. E. and Zachos, J. C.: Long-term legacy of massive carbon input to the Earth system:
Anthropocene vs. Eocene, *Philos. T. R. Soc. Lond.*, 371, 20120006, doi:10.1098/rsta.2012.0006,
2013.

Zeebe, R. E., Zachos, J. C., Caldeira, K., and Tyrrell, T.: Carbon emissions and acidification, *Science*,
321, 51–52, 2008.

1025 Zeebe, R. E., Zachos, J. C., and Dickens, G. R.: Carbon dioxide forcing alone insufficient to explain
Palaeocene-Eocene thermal maximum warming, *Nat. Geosci.*, 2, 576–580, 2009.

Table 1. Comparison of cases.

ΔV	Units	Case 1 <u>D=1kyr</u> <u>E= 1000 PgC</u>	Case 2 <u>D=100kyr</u> <u>E= 20 000 PgC</u>	Case 2 : Case 1
TC _{atm}	PgC	158.313	2123.627	13.41
TC _{ocn}	PgC	0.1681×10^4	3.0729×10^4	18.28
TA	mol	0.1354×10^{18}	2.4707×10^{18}	18.25
$\delta^{13}\text{C}_{\text{atm}}$	‰	1.009	3.550	3.52
$\delta^{13}\text{C}_S$	‰	1.036	4.775	4.61
$\delta^{13}\text{C}_M$	‰	0.686	4.955	7.22
$\delta^{13}\text{C}_D$	‰	0.873	12.188	13.96

Table 2. Summary of weathering strength variations considered.

nsi	0.20*	0.20	0.20	0.20	0.20	0.025	0.10	0.40	2.0
ncc	0.40*	0.025	0.05	0.80	2.0	0.40	0.40	0.40	0.40

* indicates LOSCAR default values.

Table 3. Variable definitions and symbols used.

Variable	Symbol	Units
Atmosphere	atm	NA
Ocean	ocn	NA
Sediments	sed	NA
High Latitude, Atlantic, Indian, Pacific Basins	H, A, I, P	NA
Surface, Intermediate, Deep Ocean Boxes	S, M, D	NA
Emissions Rate	R	PgC yr^{-1}
Emissions Duration	D	yr
Total Emissions	E	PgC
System Variable	V	Varies
Coefficient	γ	Varies
Duration Scaling Exponent	α	ND
Emissions Scaling Exponent	β	ND
Global Total Alkalinity	TA	mol
pH	pH	ND
Temperature	T	$^{\circ}\text{C}$
Sediment Carbonate Weight %	% CaCO_3	ND
Time	t	yr
Total Atmospheric Carbon	TC_{atm}	PgC
Total Oceanic Carbon	TC_{ocn}	PgC
Carbon-13 Isotope	$\delta^{13}\text{C}$	‰
Volcanic Degassing Flux	F_{vc}	PgC yr^{-1}
Air–Sea Gas Exchange Flux	F_{gas}	PgC yr^{-1}
Carbonate Weathering Flux	F_{cc}	PgC yr^{-1}
Silicate Weathering Flux	F_{si}	PgC yr^{-1}
Emissions Flux	R^f	PgC yr^{-1}
Silicate Weathering Exponent	nsi	ND
Carbonate Weathering Exponent	ncc	ND
Calcite Compensation Depth	CCD	km
Carbonate Ion	CO_3^{2-}	mol

Table 4. Power law scalings [for modern configuration](#), global variables, $\Delta V = \gamma D^\alpha E^\beta$. D in [yr] and E in [PgC].

V	Units	γ	α	β	R value
TC_{atm}	PgC	0.680 0.805	-0.32 0.289	1.22 1.174	0.986 0.98
T_{atm}	°C	0.029 2.580×10^{-2}	-0.20 0.200	0.79 0.794	0.974 0.96
TC_{ocn}	PgC	1.941 1.930	-0.003 -3.556×10^{-3}	0.98 0.982	0.999
TA	mol	1.56×10^{14} 1.561×10^{14}	-0.003 -3.467×10^{-3}	0.980 0.981	0.999
max TCO_3^{2-}	mol	1.67×10^{12} 2.021×10^{12}	1.0×10^{-5} -1.775×10^{-4}	0.99 0.965	0.995 0.99
min TCO_3^{2-}	mol	3.00×10^{14} 3.201×10^{14}	-0.23 0.209	0.77 0.736	0.855 0.89

Table 5. Power law scalings [for modern configuration](#), $\delta^{13}\text{C}$ variables, $\Delta V = \gamma D^\alpha E^\beta$. D in [yr] and E in [PgC].

V	Units	γ	α	β	R value
min $\delta^{13}\text{C}_{\text{atm}}$	‰	<u>0.087</u> <u>3.852×10^{-2}</u>	<u>-0.268</u> <u>0.242</u>	<u>0.70</u> <u>0.760</u>	<u>0.948</u> <u>0.954</u>
min $\delta^{13}\text{C}_{\text{S}}$	‰	<u>0.045</u> <u>2.907×10^{-2}</u>	<u>-0.228</u> <u>0.216</u>	<u>0.750</u> <u>0.783</u>	<u>0.969</u> <u>0.966</u>
min $\delta^{13}\text{C}_{\text{M}}$	‰	<u>0.009</u> <u>7.766×10^{-3}</u>	<u>-0.137</u> <u>0.132</u>	<u>0.81</u> <u>0.819</u>	<u>0.983</u> <u>0.979</u>
min $\delta^{13}\text{C}_{\text{D}}$	‰	<u>0.002</u> <u>1.566×10^{-3}</u>	<u>-0.035</u> <u>0.040</u>	<u>0.87</u> <u>0.877</u>	<u>0.983</u> <u>0.989</u>

Table 6. Power law scaling [for modern configuration](#), ocean boxes, $\Delta V = \gamma D^\alpha E^\beta$. D in [yr] and E in [PgC].

V	Units	γ	α	β	R value
TA _S	PgC	4.621×10^{-2}	-3.508×10^{-3}	0.982	0.999
TA _M	PgC	4.122×10^{-1}	-3.513×10^{-3}	0.982	0.999
TA _D	PgC	1.385	-3.467×10^{-3}	0.983	0.999
TA _{HL}	PgC	1.271×10^{-2}	-3.423×10^{-3}	0.982	0.999
TDIC _S	PgC	6.436×10^{-2}	-1.776×10^{-2}	0.959	0.998
TDIC _M	PgC	0.420	-3.60×10^{-3}	0.982	0.999
TDIC _D	PgC	1.454	-3.541×10^{-3}	0.982	0.999
TDIC _{HL}	PgC	1.350×10^{-2}	-4.23×10^{-3}	0.979	0.999
T_S	°C	2.473×10^{-2}	-0.196	0.795	0.964
T_M	°C	1.318×10^{-2}	-0.157	0.824	0.968
T_D	°C	4.888×10^{-3}	-0.098	0.863	0.979
min pH _S	ND	2.365×10^{-3}	-0.249	0.818	0.962
min pH _M	ND	2.050×10^{-3}	-0.211	0.799	0.940
min pH _D	ND	5.320×10^{-4}	-0.134	0.853	0.968
min CO ₂ _S	mol	5.083×10^{13}	-0.336	0.744	0.887
min CO ₂ _M	mol	2.356×10^{14}	-0.256	0.684	0.864
min CO ₂ _D	mol	1.522×10^{14}	-0.191	0.751	0.912
min CO ₂ _{HL}	mol	8.867×10^{12}	-0.289	0.711	0.894
max CO ₂ _S	mol	2.473×10^{11}	-3.223×10^{-3}	0.902	0.994
max CO ₂ _M	mol	9.146×10^{11}	-1.595×10^{-4}	0.946	0.998
max CO ₂ _D	mol	9.574×10^{11}	8.321×10^{-4}	0.980	0.998
max CO ₂ _{HL}	mol	2.013×10^{10}	-9.039×10^{-4}	0.910	0.992
max CCD _A	km	2.749×10^{-4}	-1.103×10^{-2}	0.837	0.934
max CCD _I	km	1.279×10^{-5}	-1.298×10^{-2}	1.210	0.955
max CCD _P	km	4.798×10^{-6}	-9.784×10^{-3}	1.297	0.961
min CCD _A	km	1.131×10^{-2}	-0.178	0.734	0.904
min CCD _I	km	6.233×10^{-4}	-0.220	1.046	0.896
min CCD _P	km	1.908×10^{-4}	-0.189	1.135	0.896

Table 7. Power law scalings for Paleocene/Eocene configuration, global variables, $\Delta V = \gamma D^\alpha E^\beta$. D in [yr] and E in [PgC].

V	Units	γ	α	β	R value
TC_{atm}	PgC	1.285	-0.151	1.0539	0.994
T_{atm}	°C	9.580×10^{-3}	-0.110	0.778	0.969
TC_{ocn}	PgC	1.482	-1.807×10^{-3}	0.981	0.999
TA	mol	1.130×10^{14}	-1.802×10^{-3}	0.985	0.999
max TCO_3^{2-}	mol	6.113×10^{11}	-1.954×10^{-3}	1.035	0.983
min TCO_3^{2-}	mol	4.922×10^{13}	-0.169	0.712	0.909

Table 8. Power law scalings for Paleocene/Eocene configuration, $\delta^{13}\text{C}$ variables, $\Delta V = \gamma D^\alpha E^\beta$. D in [yr] and E in [PgC].

V	Units	γ	α	β	R value
$\min \delta^{13}\text{C}_{\text{atm}}$	‰	2.005×10^{-2}	-0.199	0.777	0.963
$\min \delta^{13}\text{C}_S$	‰	1.776×10^{-2}	-0.178	0.783	0.969
$\min \delta^{13}\text{C}_M$	‰	5.243×10^{-3}	-0.099	0.819	0.981
$\min \delta^{13}\text{C}_D$	‰	1.447×10^{-3}	-0.031	0.876	0.990

Table 9. Power law scaling for Paleocene/Eocene configuration, ocean boxes, $\Delta V = \gamma D^\alpha E^\beta$. D in [yr] and E in [PgC].

V	Units	γ	α	β	R value
TA _S	PgC	0.035	-1.821×10^{-3}	0.983	0.999
TA _M	PgC	0.304	-1.837×10^{-3}	0.984	0.999
TA _D	PgC	1.013	-1.810×10^{-3}	0.985	0.999
TA _{HL}	PgC	8.414×10^{-3}	-1.730×10^{-3}	0.983	0.999
TDIC _S	PgC	0.037	-1.811×10^{-3}	0.980	0.999
TDIC _M	PgC	0.328	-1.834×10^{-3}	0.981	0.999
TDIC _D	PgC	1.103	-1.855×10^{-3}	0.982	0.999
TDIC _{HL}	PgC	9.032×10^{-3}	-1.823×10^{-3}	0.982	0.999
T_S	°C	9.180×10^{-3}	-0.108	0.780	0.969
T_M	°C	6.767×10^{-3}	-8.741×10^{-2}	0.792	0.970
T_D	°C	4.251×10^{-3}	-6.027×10^{-2}	0.812	0.976
min pH _S	ND	1.063×10^{-3}	-0.151	0.782	0.965
min pH _M	ND	8.839×10^{-4}	-0.136	0.746	0.949
min pH _D	ND	3.203×10^{-4}	-0.095	0.812	0.970
min CO ₂ _{I-S}	mol	9.639×10^{12}	-0.190	0.673	0.906
min CO ₂ _{I-M}	mol	2.637×10^{13}	-0.205	0.649	0.881
min CO ₂ _{I-D}	mol	2.537×10^{13}	-0.165	0.736	0.916
min CO ₂ _{I-HL}	mol	1.497×10^{12}	-0.184	0.672	0.908
max CO ₂ _{I-S}	mol	1.378×10^{10}	-2.215×10^{-3}	1.051	0.948
max CO ₂ _{I-M}	mol	1.914×10^{11}	-1.979×10^{-3}	1.030	0.987
max CO ₂ _{I-D}	mol	4.115×10^{11}	-2.081×10^{-3}	1.034	0.982
max CO ₂ _{I-HL}	mol	1.373×10^9	-2.000×10^{-3}	1.070	0.927
max CCD _A	km	4.563×10^{-4}	-1.441×10^{-3}	0.825	0.978
max CCD _I	km	8.724×10^{-5}	-1.214×10^{-3}	1.007	0.974
max CCD _P	km	1.772×10^{-5}	-1.833×10^{-3}	1.192	0.955
max CCD _T	km	4.472×10^{-5}	-1.784×10^{-3}	1.133	0.946
min CCD _A	km	8.918×10^{-3}	-0.124	0.666	0.911
min CCD _I	km	2.968×10^{-3}	-0.166	0.805	0.888
min CCD _P	km	1.409×10^{-4}	-0.173	1.109	0.904
min CCD _T	km	4.877×10^{-4}	-0.202	0.986	0.840

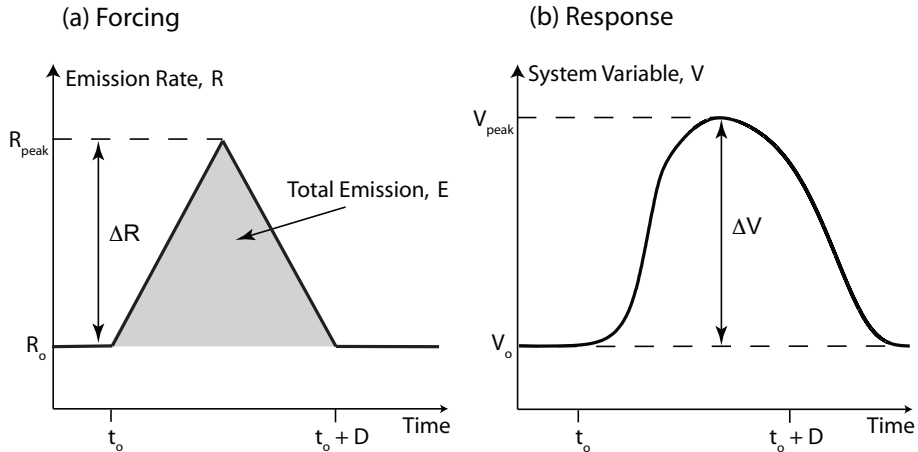


Figure 1. Schematic representations of the forcing and nature of system response. **(a)** Triangular atmospheric CO_2 perturbation characterized by duration, D , and total size of emission, E . **(b)** Typical system variable response to forcing. We define the peak system response as $\Delta V = |V_{\text{peak}} - V_0|$.

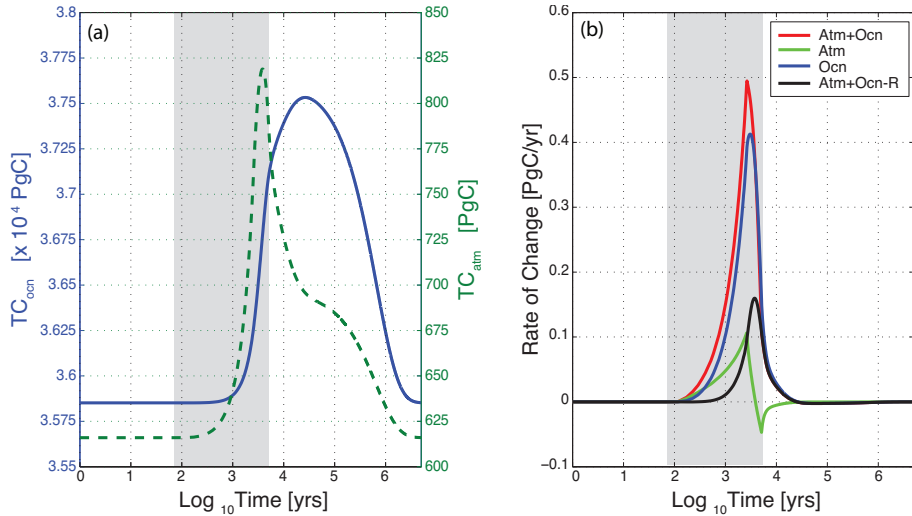


Figure 2. System response as a function of time for the case of $E = 1000$ PgC and $D = 5$ kyr. Shaded regions indicate time of emission. **(a)** Total carbon in the atmospheric and oceanic reservoirs. **(b)** Corresponding rates of change.

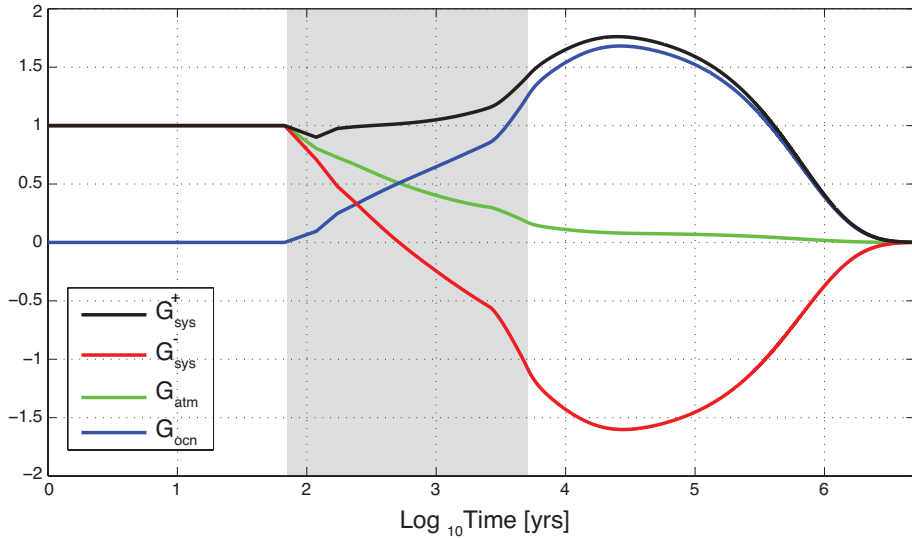


Figure 3. System gain factors as a function of time for the case of $E = 1000$ PgC and $D = 5$ kyr. Shaded region indicates time of emission.

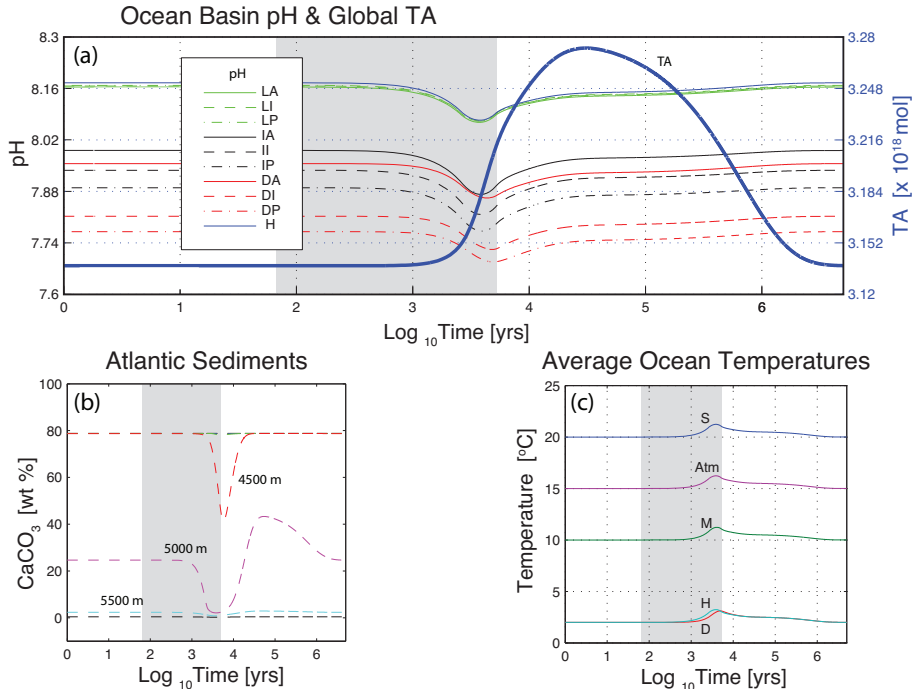


Figure 4. System variables as a function of time for the case of $E = 1000 \text{ PgC}$ and $D = 5 \text{ kyr}$. Shaded regions indicate time of emission. **(a)** Thin lines are pH for ocean boxes. Thick solid line is the global ocean total alkalinity (TA). **(b)** CaCO_3 wt % of sediment boxes within the Atlantic basin. **(c)** Temperature for atmosphere and high-latitude boxes. Surface, intermediate, and deep ocean temperatures are averages across basins.

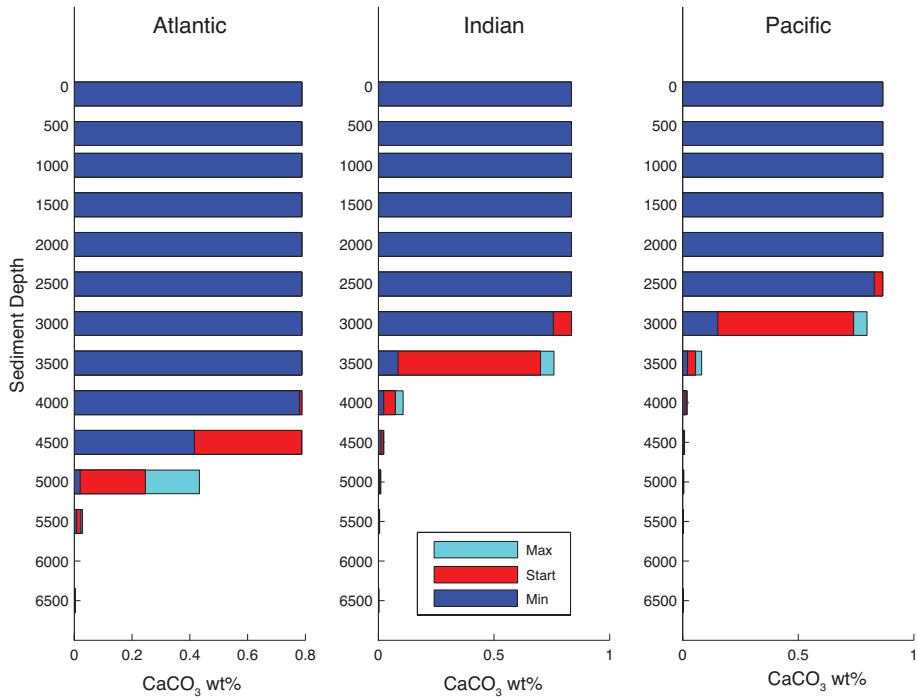


Figure 5. Extreme CaCO₃ contents in each ocean basin as a function of sediment depth for the case of $E = 1000$ PgC and $D = 5$ kyr.

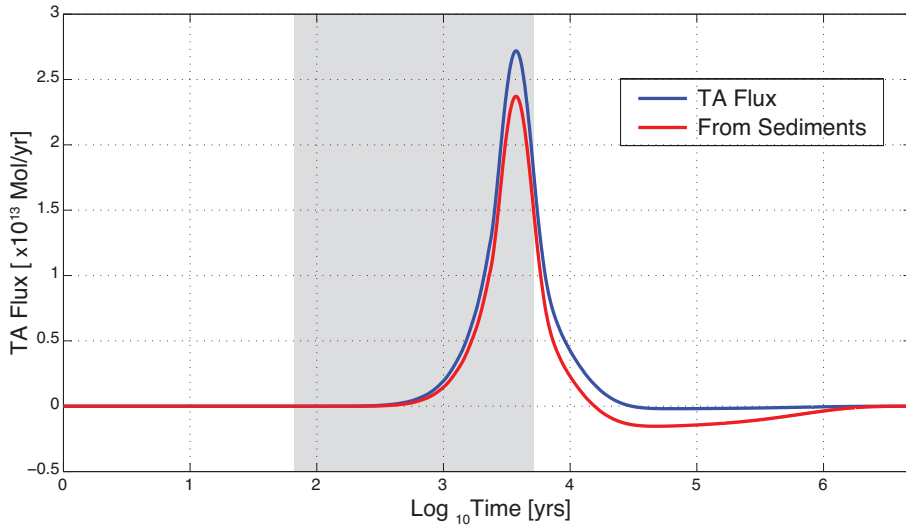


Figure 6. Time rate of change of global total alkalinity (TA) for the case of $E = 1000$ PgC and $D = 5$ kyr. Shaded region indicates time of emission. Blue curve is the time rate of change of global ocean TA. Red curve shows the blue curve minus the TA flux that is due to weathering feedbacks.

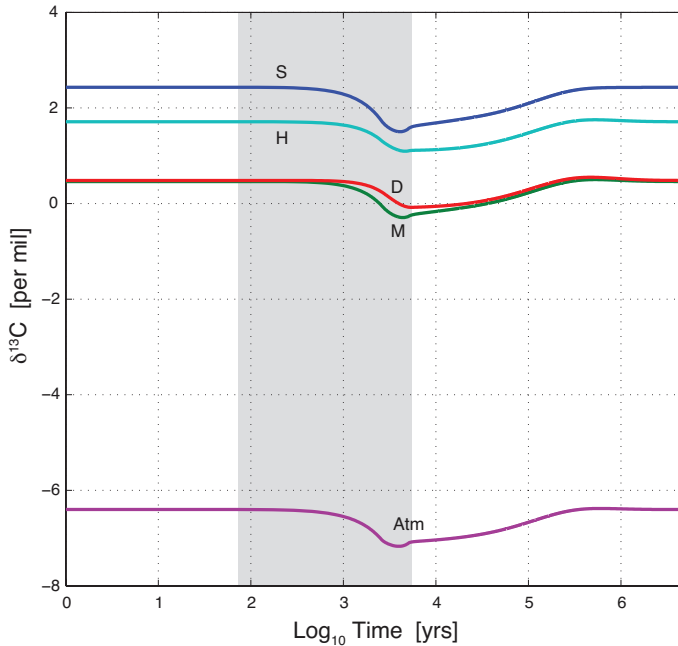


Figure 7. Carbon-13 isotope signature for the atmosphere (Atm) and ocean boxes as a function of time for the case of $E = 1000 \text{ PgC}$ and $D = 5 \text{ kyr}$. The surface (S), intermediate (M), and deep (D) boxes were averaged for all basins. H is high latitude box. Shaded region indicates time of emission.

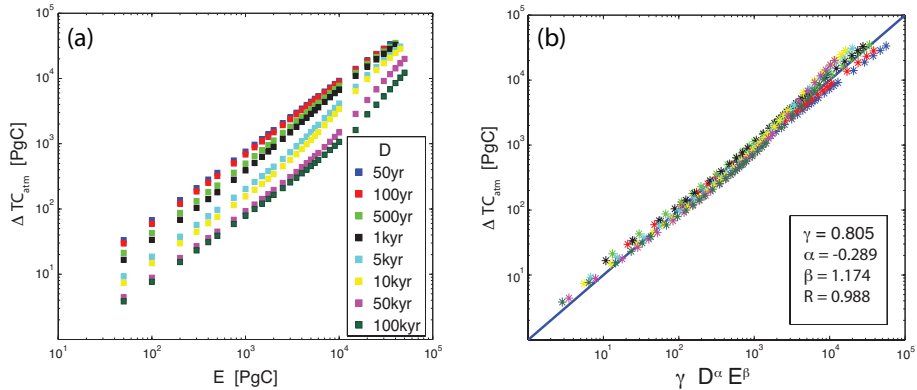


Figure 8. (a) Peak changes in the modern atmospheric total carbon content as a function of total emission, E , for various durations, D . (b) Multi-variable regression results. Solid line indicates a perfect fit to the predicted scaling. The (+) signs are each individual cases.

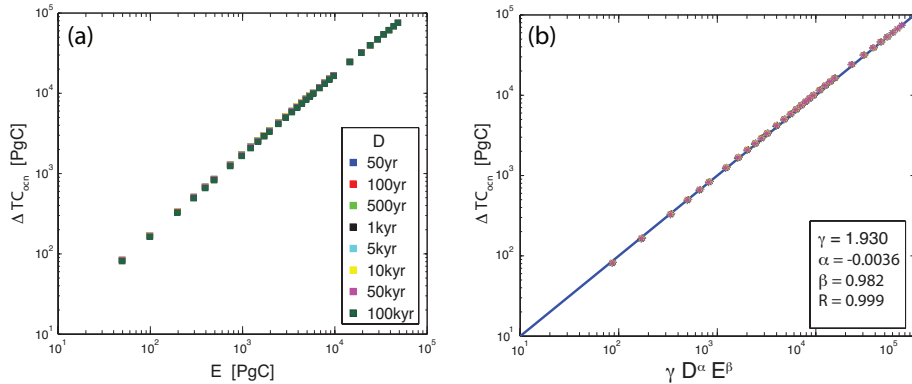


Figure 9. (a) Peak changes in the modern oceanic total carbon content as a function of total emission, E , for various durations, D . (b) Multi-variable regression results. Solid line indicates a perfect fit to the predicted scaling. The (+) signs are each individual cases.

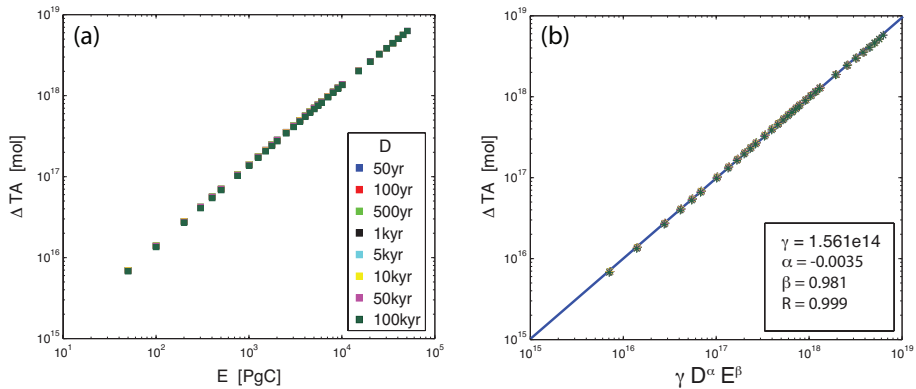


Figure 10. (a) Peak changes in the modern global ocean total alkalinity (TA) as a function of total emission, E , for various durations, D . (b) Multi-variable regression results. Solid line indicates a perfect fit to the predicted scaling. The (+) signs are each individual cases.

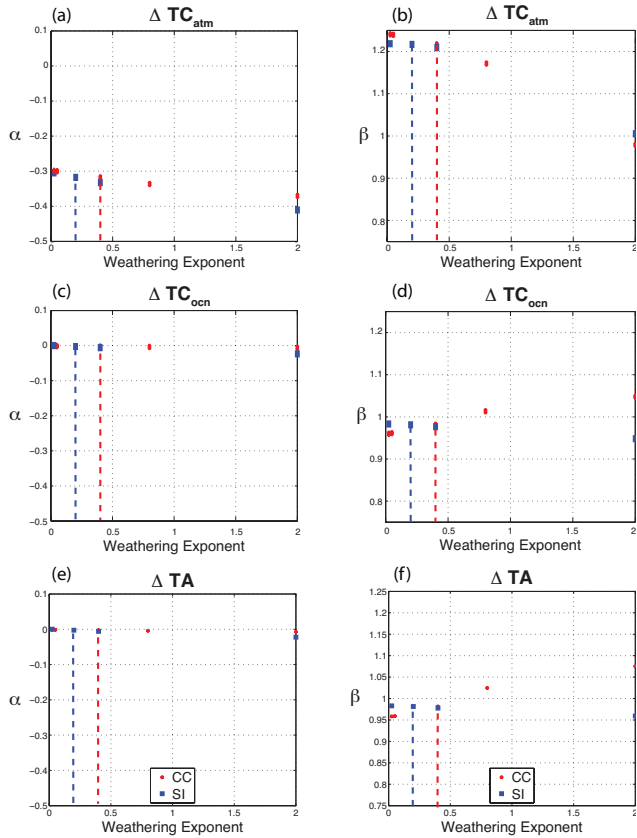


Figure 11. Sensitivity of scaling results to variations in weathering exponents. Dashed lines indicate default LOSCAR exponent values ($n_{cc} = 0.40$, $n_{si} = 0.20$). **(a, b)** Peak total atmospheric carbon, **(c, d)** peak total ocean carbon, **(e, f)** peak global total alkalinity (TA).

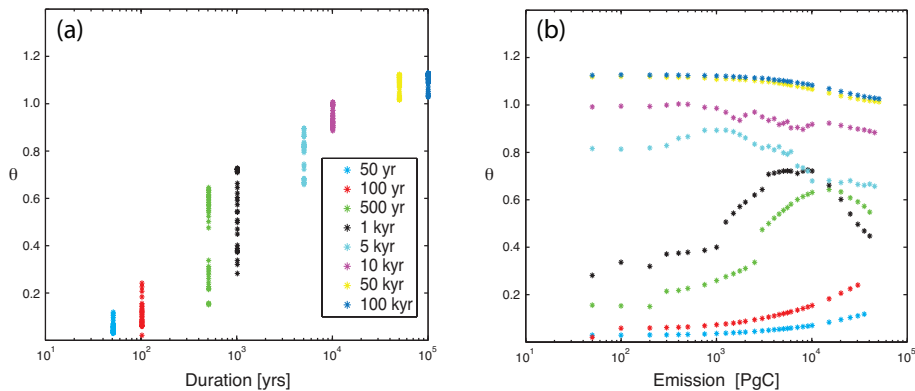


Figure 12. Ratio of the rate of change in total global dissolved inorganic carbon to the rate of change in global total alkalinity **(a)** vs. duration, at the time of maximum $p\text{CO}_2$, and **(b)** vs. emission, at the time of maximum $p\text{CO}_2$.

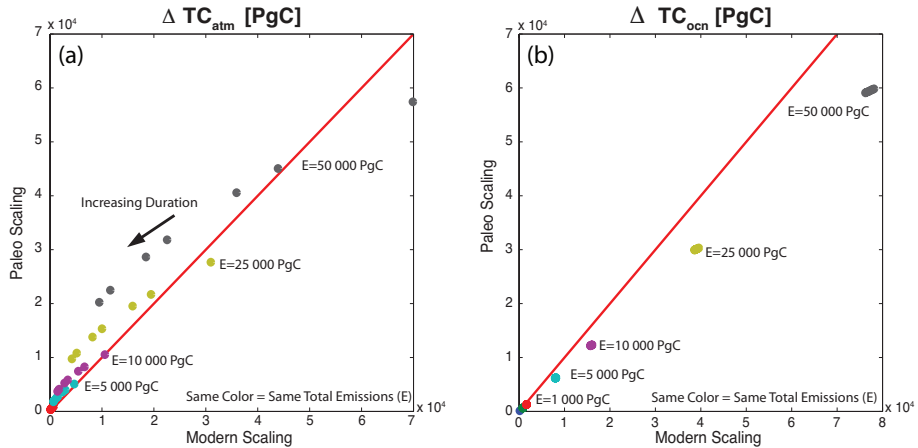


Figure 13. Correlation between peak perturbations for modern and paleo scalings. (a) Total atmospheric carbon. (b) Total oceanic carbon. Same color denotes same total emissions.

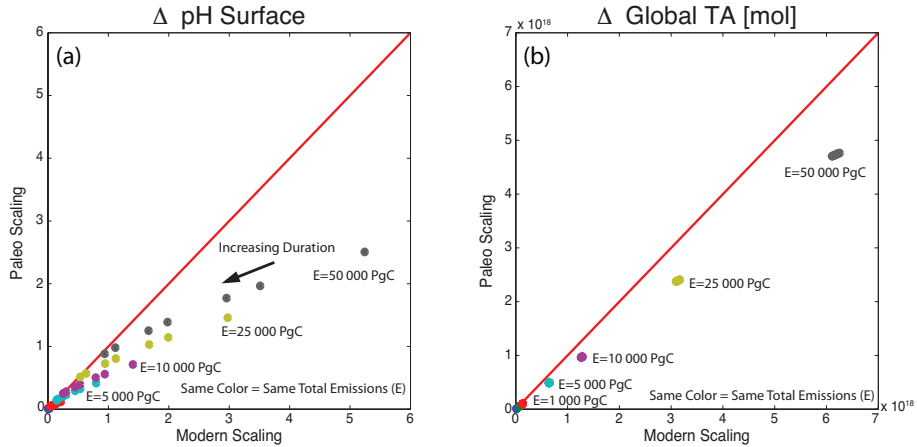


Figure 14. Correlation between peak perturbations for modern and paleo scalings. **(a)** Surface pH. **(b)** Total global alkalinity. Same color denotes same total emissions.

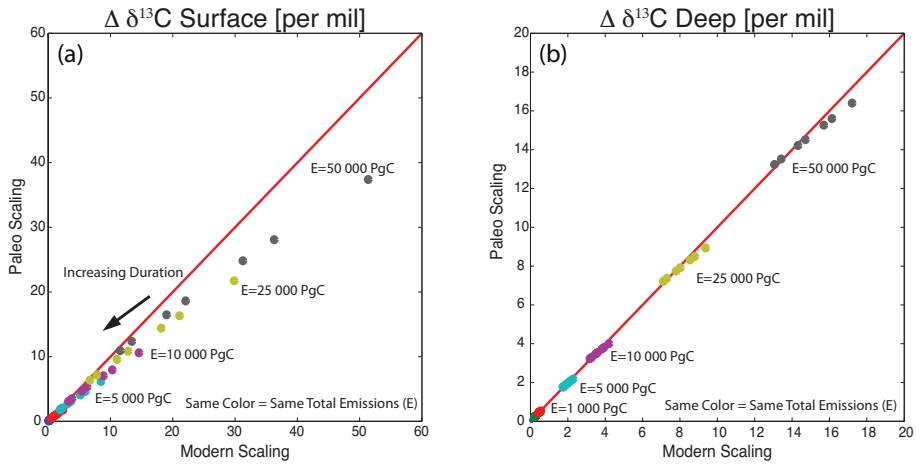


Figure 15. Correlation between peak perturbations for modern and paleo scalings. (a) Surface ocean carbon-13 anomalies. (b) Deep ocean carbon-13 anomalies. Same color denotes same total emissions.